Vascular brassinosteroid receptors confer drought resistance without penalizing plant growth

Norma Fàbregas[1,*], Fidel Lozano-Elena[1,*], David Blasco-Escámez[1], Takayuki Tohge[2,8], Cristina Martínez-Andújar[3], Alfonso Albacete[3], Sonia Osorio[4], Mariana Bustamante[1], José Luis Riechmann[1,7], Ana Conesa[5,6], Francisco Pérez Alfocea[3], Alisdair R. Fernie[2] and Ana I. Caño-Delgado[1,¶]

[1]*Centre for Research in Agricultural Genomics (CRAG) CSIC-IRTA-UAB-UB, Barcelona E-08193, Spain.*

[2]*Max Planck Institute of Molecular Plant Physiology, Potsdam-Golm D-14476, Germany.*

[3]*Department of Plant Nutrition, CEBAS-CSIC, Murcia E-30100, Spain.*

[4]*Instituto de Hortofruticultura Subtropical y Mediterránea "La Mayora". University of Malaga-Consejo Superior de Investigaciones Científicas. Department of Molecular Biology and Biochemistry, Málaga 29071, Spain.*

[5]*Microbiology and Cell Science Department, IFAS, Genetics Institute, University of Florida, Gainesville, USA.*

[6]*Genomics of Gene Expression Lab, Centro de Investigaciones Príncipe Felipe, Valencia, Spain.*

[7]*Institució Catalana de Recerca i Estudis Avançats (ICREA), Barcelona, 08010, Spain*

[8]*Current Address: NAIST Graduate school of Biological Sciences, 8916-5 Takayama, Ikoma, Nara 630-0192, Japan.*

[*] Both authors contributed equally to this work.

[¶] Correspondence to: ana.cano@cragenomica.es

ABSTRACT

Drought is the primary cause of global agricultural losses and represents a major threat to worldwide food security. Currently, plant biotechnology stands as the most promising strategy to increase crop growth in rain-fed conditions. The main mechanisms underlying drought resistance have been uncovered from the study of plant physiology and by engineering drought resistance genes into crops. However, plants with enhanced drought resistance usually display lower growth, necessitating the search for novel strategies to uncouple drought resistance from growth. Here, we show that the brassinosteroid family of receptors, in addition to promoting growth, guides the phenotypic adaptation responses to a great variety of drought stress traits herein analyzed. Whilst mutations in the ubiquitously localized BRI1 receptor pathway show an enhanced drought resistance at the expense of growth, we found that vascular-localized BRL3 receptors confer drought tolerance without penalizing overall plant growth. Systematic analyses reveal that upon drought stress the vascular BRL3 receptor pathway triggers the synthesis and mobilization of osmoprotectant metabolites, mainly proline and sugars, preferentially in the roots favoring overall plant growth. Altogether, our results uncover a new role for the spatial control of BR signaling in drought tolerance, while offer a novel strategy to address food security issues in an increasingly water limited climate.

Summary

- Brassinosteroid receptors control the plant responses to multiple drought traits in different developmental stages of roots and shoots organs.
- The vascular BRL3 receptor pathway triggers the production of osmoprotectant metabolites, preferentially sugars and proline, that once accumulated in the root help the plant to tolerate drought stress.
- BRL3 signaling promotes the transcription of canonical water stress-responses and osmoprotectant metabolism genes in normal conditions and under drought.
- Plants with increased levels of BRL3 receptors in the vascular tissues are primed and resistant to severe drought without penalizing overall plant growth.

70 **INTRODUCTION**

71 Drought causes at least 40% of crop losses worldwide and this proportion is
72 dramatically increasing due to climate change [1]. Understanding cellular responses to
73 drought stress represents the first step toward the development of better-adapted crops,
74 which is a grand challenge for plant biotechnology [2]. Classical approaches to unravel
75 how plants cope with limited water led to the identification of regulators in the signal
76 transduction cascades of the abscisic acid (ABA)-dependent [3] and ABA-independent
77 pathways [4]. Drought-stress adaptation has been associated with the presence of proteins
78 that protect cells from dehydration, such as late-embryogenesis–abundant (LEA)
79 proteins, osmoprotectants and detoxification enzymes [5-7]. These studies provided deep
80 insights into the molecular mechanisms underlying abiotic stress [2], while showing that
81 drought resistance is a complex trait simultaneously controlled by many genes. Genetic
82 approaches have succeeded in conferring stress resistance to plants, but this generally
83 comes at the cost of reduced growth [8,9]. Therefore, understanding how cellular growth is
84 coupled to drought stress responses is essential for engineering plants with improved
85 growth in rain-fed environments.

86 Receptor-Like Kinases (RLKs) play an important role in optimizing plant responses to
87 drought stress [10,11]. Brassinosteroid (BR) hormones directly bind to the BRI1 (BR-
88 INSENSITIVE 1) plasma membrane leucine-rich repeat (LRR)-RLK family members
89 [12-17]. Ligand perception triggers BRI1 interaction with the co-receptor BAK1 (BRI1
90 ASSOCIATED RECEPTOR KINASE 1) [18-20], which is essential for early BR signaling
91 events [21]. This BRI1-BAK1 heterodimerization initiates a signaling cascade of
92 phosphorylation events that control the expression of multiple BR-regulated genes
93 mainly via the BRI1-EMS-SUPPRESSOR1 (BES1) and BRASSINAZOLE
94 RESISTANT1 (BZR1) transcription factors [22-26].

95 BRs modulate multiple developmental and environmental stress responses in the plant
96 yet the role of BRs under stress conditions remains controversial. The exogenous
97 application of BRs and the overexpression of the BR biosynthetic enzyme DWF4 both
98 confer increased plant adaptation to drought stress [27-29], whereas drought resistant
99 phenotypes result from suppressing the BRI1 receptor [30,31]. Intriguingly, ABA signaling
100 inhibits the BR signaling pathway after BR perception and upstream of the BIN2
101 (BRASSINOSTEROID-INSENSITIVE 2) kinase [32,33] and further downstream crosstalk
102 is mediated by the overlapping transcriptional control of multiple BR- and ABA-
103 regulated genes [34,35], such as *RESPONSE TO DESICCATION 26* (*RD26*) [31].
104 The spatial regulation of hormonal signaling pathways is receiving increasing attention
105 in attempt to enhance understanding of coordination of plant growth and stress
106 responses [31,36-38]. The BRI1 receptor is widely localized in many tissues [39] and the
107 BRI1-LIKE receptor homologues BRL1 and BRL3 signal from the innermost tissues of
108 the plant contributing to vascular development [15,40,41]. The BR receptor complexes are
109 formed by combinations of homologous LRR-RLK receptors of the BRI1-like family
110 with the BAK1 co-receptor in the plasma membrane [41]. Despite BRI1 being a central
111 player in plant growth and adaptation to abiotic stress [31,42,43], the functional relevance of
112 vascular BRL1 and BRL3 receptors has only started to be unraveled [41,44,45]. In previous
113 proteomic approaches we identified abiotic stress-related proteins in the BRL3
114 signalosome complexes [41], yet the involvement of the BRL3 pathway in drought
115 remains elusive.
116 Here, we show that the different BR receptors modulate plant adaptation to multiple
117 drought stress traits in roots and shoots. While the traits controlled by the BRI1 pathway
118 are intimately linked to growth arrest, we found that vascular-enriched BRL3 receptors
119 confer drought resistance without penalizing overall plant growth. Metabolite profiling

120 unveils that the BRL3 signaling triggers the production of an osmoprotectant metabolite
121 signature (i.e. proline, trehalose, sucrose and raffinose family oligosaccharides) in the
122 plant, and their specific accumulation in the roots during drought periods. Subsequent
123 transcriptomic profiling shows that this metabolite signature is transcriptionally
124 regulated by BRL3 pathway in response to drought. The enrichment of deregulated
125 genes in vascular tissues, especially in the phloem, further supports the mobilization of
126 osmoprotectant metabolites to root tissues driven by BRL3 signaling under drought.
127 Overall, this study uncovers that BRL3 signaling boost sugar and osmoprotectant
128 metabolites accumulation in the root hacking drought-stress arrested growth, while offer
129 a novel strategy to protect crops from drought.
130

131 **RESULTS**

132 **BR receptors control the sensitivity to osmotic stress responses since early stages of**
133 **plant growth**

134 To investigate the contribution of the BR perception complexes to drought, we
135 performed a comprehensive characterization of different mutant combinations for all the
136 BR receptors and the BAK1 co-receptor. First, the primary root growth was analyzed
137 (Fig. 1a). Seven-day-old roots of *bak1*, *brl1brl3bak1*, *bri1* and *bri1brl1brl3* displayed
138 shorter roots than Col-0 wild-type (WT) as previously described [20,41,46,47]. We found that
139 the primary roots of the quadruple mutant *bri1brl1brl3bak1* (hereafter *quad*) were the
140 shortest and the most insensitive to BRs (Fig. 1a,b and Supplementary Fig. 1).
141 Conversely, plants overexpressing BRL3 (*35S:BRL3-GFP,* hereafter *BRL3ox*) show
142 increased receptor levels in the vascular tissues [41] and exhibited longer roots than WT
143 (Fig. 1a,b). These results are in agreement with the previously known root growth-
144 promoting role of BR receptors [46,48]. Then osmotic stress was imposed transferring

145 Arabidopsis seedlings to sorbitol-containing media and root-growth inhibition was
146 quantified relative to control conditions (methods). A significantly lesser root-growth
147 inhibition was observed in *bri1* (27%), *bri1brl1brl3* (28%) and *quad* (27%) mutants
148 when compared to WT (39%), whereas no differences were found in *brlbrl3* and
149 *bak1brl1brl3* mutant roots (Fig. 1a,b). Roots of *BRL3ox* plants were similar to WT in
150 terms of root growth inhibition under osmotic stress (Fig. 1a,b). A shorter period of
151 osmotic stress (24h) caused cell death in the elongation zone of WT roots, as marked by
152 the propidium iodine (PI) staining incorporation into nuclei [49] (Fig. 1c,d). Consistently,
153 *bri1, bri1brl1brl3* and *quad* mutants displayed reduced sensitivity to osmotic stress
154 compared to WT, as revealed by a reduced cell death in the roots (Fig. 1c,d).
155 Conversely, plants with increased levels of BRL3 receptor showed a massive cell death
156 in the root tips compared to the WT, indicating an increased sensitivity to short osmotic
157 stress treatments (Fig 1c,d). These results point to a positive role for BR receptors in
158 triggering osmotic stress responses in the plant root.
159 Since root hydrotropism represents a key feature for adaptation to water scarcity
160 environments [50,51], the capacity of the roots to escape from an imposed osmotic stress
161 bending towards water-available media was investigated (Fig. 2a). Loss-of-function
162 mutants in the BR receptors showed reduced hydrotropic responses, as roots grew
163 straighter in the sorbitol containing media than in the WT roots (Fig. 2a-c), while no
164 significant differences were found in control conditions (mock) (Supplementary Fig. 2).
165 Interestingly, *brl1brl3bak1* exhibited the most insensitive hydrotropic response to the
166 osmotic stress induction, showing lower root curvature angles than the *quad* roots (10º
167 and 16º respectively; Fig. 2b). Consistently, a hypersensitive hydrotropic response was
168 observed in *BRL3ox* (30º) compared to WT roots (24º) (Fig. 2b), whereas exogenous
169 application of the BR-synthesis inhibitor brassinazole [52] reverted the hydrotropic

170 response (Supplementary Fig. 2). A drought multi-trait matrix was generated for all the
171 BR receptor mutants analyzed in our study (Fig. 2d; Supplementary Table 1), which
172 highlights that BRL3/BRL1/BAK1 signalosome in the vascular tissues enhances
173 hydrotropic sensitivity.
174
175 **BRL3 receptors confer drought resistance without penalizing overall plant growth**
176 To investigate if the impaired responses to abiotic stress observed in root seedling were
177 preserved in mature plants, we next analyzed the phenotypes of plants exposed to severe
178 drought. After 12 days of withholding water, dramatic symptoms of drought stress were
179 observed in WT, *brl1brl3* and *brl1brl3bak1*, whereas other BR mutants showed a
180 remarkable drought resistance. In particular, *bak1*, *bri1*, *bri1brl1brl3* and *quad* mutant
181 plants were the most resistant to the severe water-withholding regime (Fig. 3a). As these
182 mutants exhibit some degree of dwarfism (Fig. 3a), survival rates after re-watering
183 drought-treated plants confirmed the resistance phenotypes (Fig. 3b). To correct for the
184 delayed plant growth of the BR deficient mutants, plants were further submitted to a
185 time-course drought stress in which water-use, photosynthesis and transpiration
186 parameters were monitored under similar relative soil water content (Fig. 3c-e). The BR
187 loss-of-function mutant plants *bri1*, *bri1brl1brl3* and *quad* took 15 days to use 70% of
188 the water available (field capacity) during the drought stress period, compared to the 9
189 days taken by WT (Fig. 3c). At similar relative soil water content, BR mutants sustained
190 higher transpiration, photosynthetic activity (Fig. 3d,e) and leaf Relative Water Content
191 (RWC) during the drought period (Supplementary Fig. 3). Altogether our results
192 indicate that the dwarf BR receptor mutant plants are more resistant while consuming
193 less water, likely through avoiding drought (Fig. 3f).

194 Strikingly, we found that *BRL3ox* plants were more resistant to severe drought stress
195 than WT plants as shown by increased survival rates (Fig. 3a,b). Plants with increased
196 BRL3 receptors reached the 70% soil field capacity two days later than the WT plants
197 (Fig. 3c). Interestingly photosynthesis rate was decreased in the *BRL3ox* at basal
198 conditions, yet it was more stable than the WT during the drought period, together with
199 transpiration. (Fig. 3d,e and Supplementary Fig. 3). These results support that BRL3
200 pathway actively promotes drought tolerance without penalizing plant growth (Fig. 3f).
201

202 **BRL3 receptors control the production of osmoprotectant metabolites**

203 To further investigate the cause of the drought tolerance conferred by BRL3 receptors,
204 we performed metabolite profiling of *BRL3ox* plants and compared it to WT and *quad*
205 plants in a time-course drought experiment. Roots were separated from shoots to
206 address possible changes in metabolite mobilization from source to sink tissues. The
207 complete metabolic fingerprints are provided in Supplementary Fig. 4 and 5 and
208 Supplementary Table 2 and 3. Metabolite profiling of *BRL3ox* mature plants grown in
209 control conditions (time 0) revealed an increment in the production of osmoprotectant
210 metabolites in the plant. Both shoots (Fig. 4a) and roots (Fig. 4c) of *BRL3ox* plants
211 exhibited a metabolic signature enriched in proline and sugars, which have been
212 previously reported to confer resistance to drought [6,53-57] suggesting that BRL3 receptor
213 promotes priming [58,59]. Importantly, those metabolites were decreased in *quad* mutant
214 plants (Fig. 4a,c).

215 The sugars fructose, glucose, galactinol, galactose, maltose and raffinose were
216 accumulated in *BRL3ox* shoots (Fig. 4a). Conversely, sucrose, trehalose, *myo*-inositol
217 and maltose were accumulated in *BRL3ox* roots, while glucose levels were decreased
218 (Fig. 4c). The fact of increased glucose and fructose levels in the shoots while higher

219 levels of sucrose levels in the roots suggest that BRL3 pathway promotes sugar
220 mobilization to the roots (Fig. 4a). In response to drought, the dynamics of each
221 metabolite was analyzed along a time-course [60]. A rapid mobilization of osmoprotectant
222 metabolites was observed in *BRL3ox* plants (Fig. 4b,d). In shoots exposed to drought,
223 proline showed the highest levels respect WT along the entire drought time course (Fig.
224 4b,f). Instead, glucose, galactose and *myo*-inositol increased at similar or lower rates in
225 *BRL3ox* than in WT plant shoots (Fig. 4e,g). However in roots, an accumulation of
226 trehalose, sucrose, proline and raffinose was observed in *BRL3ox* under drought stress
227 time-course (Fig. 4d), following a steeper exponential dynamics than in WT plants (Fig.
228 4h). Additionally glucose, galactose, fructose and *myo*-inositol were linearly increased
229 in WT while exponentially accumulated in *BRL3ox* roots (Fig. 4j). Interestingly, along
230 the drought-time course these metabolite levels were decreased in the *quad* mutant
231 plants, compared to WT (Supplementary Fig. 6). Together, the drought time course
232 metabolite profiling uncovers a key role of BR receptors in promoting sugar metabolism
233 while supports that BRL3 triggers the accumulation of osmoprotectant metabolites in
234 the root, promoting growth under drought conditions.
235
236 **BRL3 transcriptional control of metabolite production in response to drought**
237 The osmolyte accumulation observed in roots of plants with increased BRL3 receptor
238 levels suggested a faster sugar mobilization from shoot to roots. We next investigated
239 whether those metabolic pathways were regulated transcriptionally by BRL3 in the root.
240 RNAseq of *BRL3ox* roots revealed 759 genes deregulated at basal conditions (214 up
241 and 545 down; FC>1.5, FDR<0.05; Fig. 5a; Supplementary Table 4) and 1068 genes
242 deregulated in drought conditions (378 up and 690 down; FC>1.5, FDR<0.05; Fig. 5a,
243 Supplementary Table 4). Both sets of deregulated genes overlapped only a 13% (Fig.

244 5c). In control conditions, a high proportion of deregulated genes were annotated in GO
245 category of response to water stress, oxygen-containing compounds (ROS) and
246 response to ABA (Fig. 5d, 5e, Supplementary Table 5). We next classified the genes in
247 the response to stress category, which included classical drought stress markers such as
248 *RD22* or *RAB18* already upregulated in basal conditions (Fig 5b). The enrichment of
249 response to hormone genes indicated altered hormonal responses in *BRL3ox* plants (Fig
250 5d). Further analyses of specific hormonal pathways revealed ABA and jasmonic acid
251 (JA) as the most altered responses (Supplementary Fig. 7). Repression of the JA
252 signaling and synthesis genes resulted in decreased levels of JA in basal conditions
253 (Supplementary Fig. 7). An exclusive GO category being overrepresented in drought
254 was cell wall organization. Enzymes that down-regulated in *BRL3ox* under drought
255 (Fig. 5e) included a nourished group of expansins, pectin-lyases and cell wall
256 invertases, suggesting that *BRL3ox* plants are able to guarantee a sugar supply to the
257 root and keep cell wall integrity upon drought (Supplementary Fig. 8).
258 Analysis of transcription factors (TF) showed 29 TFs with differential response to
259 drought between *BRL3ox* and WT roots. Interestingly, the drought-responsive TF *RD26*
260 showed and enhanced response in *BRL3ox* roots during stress, whereas several vascular-
261 specific TFs upon drought remained repressed (Supplementary Fig. 9).
262 Given that the native expression domain of BRL3 receptor is located at phloem-pole
263 pericycle and the enriched localization in vascular tissues when overexpressed [41], the
264 spatial distribution of deregulated genes in the root tissues was analyzed in our RNAseq
265 dataset [61]. The deregulated genes were preferentially enriched in vascular tissues, such
266 as phloem and pericycle, but also in lateral root primordia and root hair cells, especially
267 during the drought stress (Fig. 6a,b, See methods). Among phloem-enriched genes we
268 found two galactinol synthases (*GolS*) and trehalose phosphatases (*TPPs*) with

269 increased expression in *BRL3ox* roots both, in basal conditions and drought (Fig. 6 c, d).
270 These enzymes drive the synthesis of the osmoprotectant metabolites trehalose, myo-
271 inositol and raffinose we found accumulated in *BRL3ox* roots. Together, these results
272 support the importance of BRL3 signaling in the phloem to sustain drought resistance.
273 Furthermore, by statistical analysis a significant link between the whole transcriptomic
274 and metabolomic signatures was found, both in basal conditions and under drought
275 (p=0.017 and p=0.001 respectively, methods), indicating that the metabolic signature of
276 *BRL3ox* plants is transcriptionally controlled. We used the metabolic and transcriptomic
277 signatures to identify deregulated metabolic pathways using Paintomics [62]. The analysis
278 revealed a constitutive control of sucrose metabolism by the vascular BRL3 pathway
279 that sustained during drought stress. We also found that BRL3 controls the galactose
280 metabolism under drought, which includes the Raffinose Family of Oligosaccharides
281 (RFOs) synthesis pathway (Supplementary Fig. 10, Supplementary Table 8).
282 Collectively, these results support that BRL3 receptor promotes drought tolerance,
283 mainly controlling sugar metabolism.
284

285 **DISCUSSION**

286 Our study address the importance of vascular BRL3 signaling in the transcriptional
287 control of metabolic pathways responsible for the production of osmoprotectant
288 metabolites in the leaves, that are mobilized to the roots preventing growth arrest during
289 severe drought periods (Supplementary Fig. 11). Spatial BR signaling has been shown
290 to contribute to stem cell replenishment in response to genotoxic stress[36,37], while the
291 present study uncovers a role for vascular-enriched BRL3 receptors in promoting
292 growth during drought periods. Together, these results show the importance of the

293 spatial regulation of BR signaling in plant stress responses and open a new window for
294 the study of drought tolerance with cell-specific resolution in plants.
295 Exogenous application of BR compounds has been widely used in agriculture to extend
296 growth under different abiotic stresses [27,30,63], yet how these molecules precisely are
297 able to activate growth in challenging conditions remains largely unknown. The
298 analysis of BR signaling and synthesis mutant plants in responses to stress failed to
299 provide a linear picture for their involvement in drought stress adaptation. The
300 overexpression of the canonical BRI1 receptor pathway and the BR-biosynthesis gene
301 DWF4 can both confer abiotic stress resistance [29,43] whereas *BRI1* loss-of-function
302 mutants also showed drought stress resistance [31]. However, increased levels of BR-
303 regulated transcription factors trigger antagonistic effects in drought stress responses
304 [31,64], thus depicting a complex scenario for BRs role on abiotic stress. Given the
305 spatiotemporal regulation of the BR-signaling components [45] and the complexity of
306 drought traits [9], it is plausible to hypothesize that drought traits are under control of cell-
307 type specific BR-signaling.
308 Our study unveils that the BR family of receptors, in addition to promoting growth,
309 guides the phenotypic adaptation responses to a myriad of drought stress traits. The
310 drought resistance phenotypes of BR loss-of-function mutants (Fig. 3a) are likely
311 caused by drought avoidance linked to growth arrest and a stress-insensitivity that
312 maintains transpiration, leaf water status and photosynthesis (Fig. 3e,f). The reduced
313 levels of ABA and canonical stress related metabolites together with the down-
314 regulation of drought stress genes further support the *quad* plants insensitivity to stress
315 (Supplementary Figs. 6 and 7). We found the drought-response RD26 transcription
316 factor expression enhanced in *BRL3ox* roots upon drought (Supplementary Fig. 9).
317 RD26 was shown to antagonize with the BRs canonical TF BES1 [31], thus suggesting

318 alternative pathways being activated by BRL3. The alternative pathways may be
319 derived of a spatial specialization of the BR functions within the root. Indeed we found
320 enriched transcriptional responses in the vascular tissues of the *BRL3ox* roots, especially
321 within phloem-related cell types (Fig. 6a,b). The native expression domain of BRL3 and
322 the metabolic signature profile found in *BRL3ox* supports the hypothesis of its
323 implication in phloem loading during drought. Moreover metabolic enzymes implicated
324 in trehalose and RFO metabolism were enriched in vascular tissues and upregulated in
325 *BRL3ox* roots (Fig. 6c,d). Thus, BRL3 function is not limited to the phloem
326 loading/unloading but also directly controlling metabolic pathways. Such is the case of
327 trehalose phosphate phosphatase family (*TPPs*) [65-67] and galactinol synthase 2 (*GolS2*)
328 [68-70], involved in trehalose and RFOs synthesis respectively, which have been described
329 to impact drought responses. In addition to the vascular findings, our analysis uncover
330 the control of non-vascular enzymes important in metabolism and drought responses, i.e
331 the control of hexokinases such as *HXK3* or *HKL1* and sucrose synthases, *SUS3* and
332 *SPS2F* or the constitutive downregulation of proline dehydrogenase genes, as the early
333 response to dehydration 5 (*ERD5)* [71,72]. In light of our findings, we propose that
334 vascular BRL3 receptors action may partially occur independently of the canonical
335 growth-promoting BRI1 pathway, given the drought hypersensitivity found in *Bes1-D*
336 gain-of-function mutants [31].
337 Our data further suggest that *BRL3ox* plants accumulate sugars in sink tissues to provide
338 plant root growth to escape drought by searching for water in the soil. Supporting these
339 findings, reduced photosynthesis was observed in the well-watered *BRL3ox* plant shoots
340 (Fig. 3e). These results, together with the higher levels of sucrose levels in roots over
341 shoots (Fig. 4a) suggest that the BRL3 pathway promotes sugar mobilization from the
342 leaves (source) to the roots (sink). Previous work reported that BRs promote the flow of

343 assimilates from source to sink via the vasculature [73] and sucrose phloem unloading [74]
344 in crops.
345 In control conditions *BRL3ox* plants exhibited a metabolic signature enriched in proline
346 and sugars. Proline and sugars accumulation classically correlates with drought stress
347 tolerance, osmolyte, ROS scavenger and chaperone functions [6,53-57] suggesting that
348 BRL3 receptor promotes priming [58,59]. In addition, *BRL3ox* plants also accumulated
349 succinate, fumarate and malate. Importantly, all these metabolites were decreased in
350 *quad* mutant plants. Altogether, these metabolic data uncover a role of BR signaling in
351 promoting the tricarboxylic acid (TCA) cycle, sugar and amino acid metabolism [75].
352 In drought stress conditions, *BRL3ox* shoots displayed increased levels of the amino
353 acids proline, GABA and tyrosine. In the *BRL3ox* roots, trehalose, sucrose, *myo*-
354 inositol, raffinose and proline were the most accumulated metabolites along the stress
355 time course, and all have previously been linked to drought resistance [53-55]. In addition,
356 the RFO metabolites raffinose and *myo*-inositol, involved in membrane protection and
357 radical scavenging [76], were increased in *BRL3ox,* yet reduced in *quad* mutant roots
358 under drought.
359 Our data thus indicate that *BRL3ox* roots are loaded with osmoprotectant metabolites,
360 thus better prepared to alleviate drought stress, via a phenomenon previously referred to
361 as priming [58,59]. Further supporting our hypothesis, the BRL3 signalosome is enriched in
362 abiotic stress proteins [41]. Altogether these data suggest that sensing drought stress
363 responses is correlated with BRL3 receptor levels in the root vasculature, especially in
364 the phloem [77] is key in contributing to greater survival rates in *BRL3ox* shoots. Future
365 cell-type specific engineering of signaling cascades stands as promising strategy to
366 surpass the growth arrest caused by drought stress.
367

368 **METHODS**

369 **Plant materials**

370 Seeds were sterilized with 35% NaClO for 5 min and washed 5 times for 5min with
371 sterile dH_2O. Sterile seeds were vernalized 48 h at 4ºC and grown in half-strength agar
372 Murashige and Skoog (MS1/2) media with vitamins and without sucrose. Plates were
373 grown vertically in long day (LD) conditions (16 h of light / 8 h of dark; 22°C, 60%
374 relative humidity). Genotypes used in this study: Columbia-0 WT (Col-0 WT), *brl1-*
375 *1brl3-1* (*brl1brl3*), *bak1-3* (*bak1*), *bri1-301* (*bri1*), *bri1-301brl1-1brl3-1* (*bri1brl1brl3*),
376 *bri1-301bak1-3brl1-1brl3-1 (quad)* and *35S:BRL3-GFP (BRL3ox)* [41]. DNA rapid
377 extraction protocol [78] was used for all the plant genotyping experiments. Primers used
378 for genotyping the BR mutant plants are described in Table 1.

379

380 **Brassinolide and sorbitol sensitivity assays in roots**

381 For hormone treatments, seeds were continuously grown in concentrations series of
382 brassinolide (BL,Wako, Japan). For sorbitol assays, three-day-old seedlings were
383 transferred to either control or 270mM sorbitol media four additional days. Seven-day-
384 old seedlings root length was measured with Image J (http://rsb.info.nih.gov/ij/) and
385 compared to automatically acquired data with MyROOT [79] software (Supplementary
386 Fig. 12). Four-day-old roots grown in control conditions or in 24h of sorbitol treatment
387 were stained with Propidium iodide (10ug/ml, PI, Sigma) that stains the cell wall
388 (control) and DNA in the nuclei upon cell death (sorbitol). Images were acquired with
389 confocal microscope (FV1000 Olympus). Cell death damage in primary roots was
390 measured in a window of 500µm from QC in the middle root longitudinal section
391 (Image J). As arbitrary setting to measure the stained area, a color threshold ranging
392 from 160 to 255 in brightness was selected.

393

394 **Root hydrotropism**

395 Seedlings were germinated in MS1/2 for six days. The lower part of the plates was
396 removed and MS1/2 with 270mM sorbitol was added, to simulate a situation with
397 reduced water availability. 1μM of BRZ_{220} [80] was added to sorbitol media when
398 indicated. The media was placed in 45-degree angle to scape gravitropism effect as
399 previously described [50,51]. Root curvature angles were measured and analyzed with
400 Image J software (http://rsb.info.nih.gov/ij/).

401

402 **Drought stress for scoring plant survival**

403 One-week-old seedlings grown in MS1/2 agar plates were transferred individually to
404 pots containing 30±1 g. of substrate (plus 1:8 v/v vermiculite and 1:8 v/v perlite). For
405 each biological replicate, 40 plants of each genotype were grown in LD conditions for
406 three weeks. Three-week-old plants were subjected to severe drought stress by
407 withholding water during 12 days followed by re-watering. After the 7 days of recovery
408 period, the surviving plants were pictured and manually counted (two-sided chi-squared
409 test, $P<0.01$).

410

411 **Metabolite profiling analyses**

412 One-week-old seedlings were placed in individual pots with 30g of autoclaved soil and
413 grown in LD photoperiodic conditions. After 3 weeks growing, half of plants were
414 subjected to a severe drought period of six days (withholding water) and other half were
415 watered normally (well-watered control conditions). A total of five biological replicates
416 were collected every 24h during the time course (from day 0 to day 6) both in drought
417 and watered conditions for each genotype (WT, *quad* and *BRL3ox*). Four independent

418 plants were bulked in each biological replicate. Roots were manually separated from
419 shoots. Root samples were aliquoted in 20mg and shoot samples in 50mg (exact weight
420 was annotated for data normalization). Primary metabolites extraction was carried as
421 previously described [81]. Samples were transferred into glass vials specific for injection
422 in GC-TOF-MS. The GC-TOF-MS system comprised a CTC CombiPAL autosampler,
423 an Agilent 6890N gas chromatograph, and a LECO Pegasus III TOF-MS running in EI+
424 mode. Metabolites were identified in comparison to database entries of authentic
425 standards [82]. Chromatograms were evaluated using Chroma TOF 1.0 (Leco) Pegasus
426 software for peak identification and correction of RT. Mass spectra were evaluated
427 TagFinder 4.0 software [83] for metabolite annotation and quantification (peak area
428 measurements). The resulting data matrix was normalized using an internal standard
429 Ribitol in 100% Methanol (20:1) followed by normalization with the fresh weight of
430 each sample. Control well-watered conditions (day 0) metabolomic data was analyzed
431 with a two-tailed t-test, p-value<0.05 (no multiple testing correction). Time course
432 analysis data was analyzed with R software, using maSigPro package [60]. Briefly the
433 profile of each metabolite in each condition was fitted to a polynomial model of
434 maximum degree 3. Statistical comparison of curves between genotypes was done
435 taking into account the fitting value, then the p-value was corrected (Benjamini-
436 Hochberg method) and significant metabolites (p-value < 0.05) having a differential
437 profile between genotypes were plotted to visualize their behavior under the drought
438 time course. Clustering analysis was done by maSigPro package itself, using the *hclust*
439 R core function.
440
441 **Transcriptomic profiling analysis**

442 For microarray analysis, a drought stress time-course analysis was carried in WT and
443 *quad* mutant three-week-old mature plants. Entire plants were collected every 48 hours
444 during the time course (Day 0, Day 2 and Day 4) under drought stress and control
445 conditions. Two biological replicates composed of 5 independent rosettes were
446 collected. RNA was extracted with Plant Easy Mini Kit (Qiagen) and quality checked
447 by Bioanalyser. Genome-Wide Microarray platform (Dual color, Agilent) was done by
448 swapping color hybridization of each biological replicate (Cy3 and Cy5). Statistical
449 analysis was performed with the package "limma" [84], the "mle2/"normexp" background
450 correction method was used. Quantile normalization was used to normalize different
451 microarrays then a Bayes test was used to identify differentially expressed probes. The
452 results were filtered for adjusted p-value<0.05 (after Benjamini-Hochberg correction)
453 and Log2 FC >|1.5|. For RNAseq analysis, three-week-old roots were detached from
454 mature plants grown on soil at control conditions and exposed to 5 days of drought.
455 RNA was extracted as described above. Stranded cDNA libraries were prepared with
456 TruSeq Stranded mRNA kit (Illumina). Single-end sequencing, with 50-bp reads, was
457 performed in an Illumina HiSeq500 sequencer, at a minimum sequencing depth of 21M.
458 Reads were trimmed 5bp at their 3' end and quality filtered then mapped against the
459 TAIR10 genome with "HISAT2". Mapped reads were quantified at gene level with
460 "HtSeq". For differential expression samples were TMM normalized and statistical
461 values calculated with "EdgeR" package in R. Results were filtered for adjusted p-value
462 (FDR) <0.05 and FC >|2|. Heatmap representations were performed in R with the
463 heatmap.2 function implemented in the "gplots" package.
464
465 **Statistical methods and metabolic and transcriptomic data integration.**

466 For root tissue enrichment analysis, deregulated genes were queried against available
467 tissue-enriched genes lists [61]. For each tissue, a 2x2 contingency table was constructed
468 counting for the number of deregulated genes enriched and not enriched in the tissue
469 and also for the number of not deregulated genes (for either FDR>0.05 or logFC >/< in
470 the RNAseq gene universe) enriched and not enriched in the tissue. Statistical value of
471 the enrichment was obtained with one-sided Fisher's test. To statistically evaluate the
472 influence of transcriptomic changes in the metabolic signature, both deregulated
473 enzymes and metabolites were queried in an annotation file for Arabidopsis thaliana's
474 metabolic reactions, which included merged data from KEGG
475 (http://www.genome.jp/kegg/) and BRENDA (www.brenda-enzymes.org) databases.
476 Then same approach of constructing a 2x2 contingency table was taken. Significant and
477 not significant metabolites annotated in the database were matched with differential or
478 not differential expressed genes annotated in the database. The statistical value of the
479 association between regulated metabolites and genes was obtained through a two-sided
480 Fisher's exact test. Genes and metabolites were mapped into the KEGG pathways using
481 the PaintOmics3 (http://bioinfo.cipf.es/paintomics/) according the developer
482 instructions [62].
483
484 **Physiological analysis and Chlorophyll fluorescence parameters**
485 One-week-old seedlings were placed in individual pots and watered with the same
486 volume of a modified one-fifth-strength Hoagland solution. Pots were weighed daily
487 during the experiment. Well-watered control plants were grown at 100% of field
488 capacity (0% of water loss). Time-course drought stress assay started by withholding
489 nutrient solution until reaching 25, 50, 60 and 70% of water loss. Photosynthesis (*A*)
490 and transpiration (*E*) were measured in control and drought plants at those time points.

491 Four plants of each genotype were harvested at 0, 50 and 70% of water loss for biomass,
492 water content and hormone analyses. Drought experiments were repeated three times
493 and at least 4 plants per genotype and treatment were used in each experiment. RWC
494 was calculated according to the formula: RWC (%) = [(FW-DW) / (TW-DW)] x 100.
495 Plant hormones cytokinins (*trans*-zeatin), gibberellins (GA1, GA4 and GA3), indole-3-
496 acetic acid (IAA), abscisic acid (ABA), salicylic acid (SA), jasmonic acid (JA) and the
497 ethylene precursor 1-aminocyclopropane-1-carboxylic acid (ACC) were analyzed in the
498 leaves as previously described [85].
499

500 **ACKNOWLEDGEMENTS**

501 We acknowledge financial support from the Spanish Ministry of Economy and
502 Competitiveness, through the "Severo Ochoa Programme for Centres of Excellence in
503 R&D" 2016-2019 (SEV-2015-0533)", the CERCA Programme from the Generalitat de
504 Catalunya, and the Agencia de Gestió d'Ajuts Universitaris i de Recerca (2014 SGR
505 1406). N.F. is funded by Fundación Renta Corporación and by EMBO short-term
506 postdoctoral fellowship (ASTF 422-2015). F.L.E and D.B are funded by BIO2013-
507 43873 grant from the Spanish Ministry of Economy and Competitiveness in A.I.C.-D.
508 laboratory. CMA, AA and FPA acknowledge financial support from the Spanish
509 MINECO-FEDER (project AGL2014-59728-R) and from the European Union's
510 Seventh Framework Programme for research technological development and
511 demonstration under grant agreement no. 289365 (project ROOTOPOWER). SO was
512 supported by Ministry of Science and Innovation and University of Malaga (Spain)
513 through the grant Ramón and Cajal program (Sonia Osorio, RYC-09170). M.B and
514 J.L.R are supported by grant BFU2014-58289-P from the Spanish Ministry of Economy
515 and Competitiveness. A.C.D. – A.C. collaboration was funded by the European

516 Regional Development Funds and Marie Curie IRSES Project DEANN (PIRSES-GA-
517 2013-612583). A.I.C.-D. is a recipient of a BIO2013-43873 grant from the Spanish
518 Ministry of Economy and Competitiveness and European Research Council, ERC
519 Consolidator Grant (ERC-2015-CoG – 683163).

520

521 **AUTHOR CONTRIBUTIONS**

522 A.I.C.-D conceived, designed and supervised the study. N.F., F.L.E, D.B., C.M.A. and
523 F.P.A. performed the genetics and stress phenomic experiments and data analyses. N.F.,
524 F.L.E., M.B., J.L.R. and A.C.D. designed the genome-wide experiments. N.F., F.L.E.,
525 A.C. and A.C.D. performed the genome-wide experiments and data analysis. N.F.,
526 F.L.E., T.T., S.O., and A.R.F. carried out the metabolite and data analysis. A.A.
527 performed the hormone profiling experiments. N.F. and A.C.D. wrote the manuscript.
528 All authors discussed the results and the manuscript.

529

530 **Table 1. Primers used for genotyping**

primer	**Sequence (5' - 3')**	**Mutant**
bri2.11	GTGAGAAACGAAGGTGGAACAGACTGCAG	*brl1-1*
bri2.12	CTTCTTGGCATGGATACGGGAGGTAATGG	*brl1-1*
JMLB	GGCAATCAGCTGTTGCCCGTCTCACTGGTG	*brl1-1*
bri4.2	TTTAGGGTGAGCATGAGATCTCGTGGGCCG	*brl3-1*
bri4.3	GAAATCCCTGTAGGAATCGGAAAGCTTGAG	*brl3-1*
JMRB	GCTCATGATCAGATTGTCGTTTCCCGCCTT	*brl3-1*
bak1-3 F	GCACTGAAAAACAGTTTAGC	*bak1-3*
bak1-3 R	GATGCAGGAAGGGGAGTCAACTTGGTG	*bak1-3*
T-DNA R	GCGTGGACCGCTTGCTGCAACT	*bak1-3*
bri1-301 F	GGAAACCATTGGGAAGATCA	*bri1-301* *
bri1-301 R	GCTGTTTCACCCATCCAA	*bri1-301* *

531 *PCR product was digested by *DpnII* enzyme (R0543, New England Biolabs)

532 **REFERENCES**

533 1 Boyer, J. S. Plant productivity and environment. *Science* **218**, 443-448,
534 doi:10.1126/science.218.4571.443 (1982).
535 2 Todaka, D., Shinozaki, K. & Yamaguchi-Shinozaki, K. Recent advances in the
536 dissection of drought-stress regulatory networks and strategies for development
537 of drought-tolerant transgenic rice plants. *Front Plant Sci* **6**, 84,
538 doi:10.3389/fpls.2015.00084 (2015).
539 3 Cutler, S. R., Rodriguez, P. L., Finkelstein, R. R. & Abrams, S. R. Abscisic acid:
540 emergence of a core signaling network. *Annu Rev Plant Biol* **61**, 651-679,
541 doi:10.1146/annurev-arplant-042809-112122 (2010).
542 4 Yoshida, T., Mogami, J. & Yamaguchi-Shinozaki, K. ABA-dependent and
543 ABA-independent signaling in response to osmotic stress in plants. *Curr Opin*
544 *Plant Biol* **21**, 133-139, doi:10.1016/j.pbi.2014.07.009 (2014).
545 5 Graether, S. P. & Boddington, K. F. Disorder and function: a review of the
546 dehydrin protein family. *Front Plant Sci* **5**, 576, doi:10.3389/fpls.2014.00576
547 (2014).
548 6 Seki, M., Umezawa, T., Urano, K. & Shinozaki, K. Regulatory metabolic
549 networks in drought stress responses. *Curr Opin Plant Biol* **10**, 296-302,
550 doi:10.1016/j.pbi.2007.04.014 (2007).
551 7 Umezawa, T. *et al.* CYP707A3, a major ABA 8'-hydroxylase involved in
552 dehydration and rehydration response in Arabidopsis thaliana. *Plant J* **46**, 171-
553 182, doi:10.1111/j.1365-313X.2006.02683.x (2006).
554 8 Shao, H. B., Chu, L. Y., Jaleel, C. A. & Zhao, C. X. Water-deficit stress-induced
555 anatomical changes in higher plants. *C R Biol* **331**, 215-225,
556 doi:10.1016/j.crvi.2008.01.002 (2008).
557 9 Tardieu, F. Any trait or trait-related allele can confer drought tolerance: just
558 design the right drought scenario. *J Exp Bot* **63**, 25-31, doi:10.1093/jxb/err269
559 (2012).
560 10 Marshall, A. *et al.* Tackling drought stress: receptor-like kinases present new
561 approaches. *Plant Cell* **24**, 2262-2278, doi:10.1105/tpc.112.096677 (2012).
562 11 Smakowska-Luzan, E. *et al.* An extracellular network of Arabidopsis leucine-
563 rich repeat receptor kinases. *Nature* **553**, 342-346, doi:10.1038/nature25184
564 (2018).
565 12 Clouse, S. D., Langford, M. & McMorris, T. C. A brassinosteroid-insensitive
566 mutant in Arabidopsis thaliana exhibits multiple defects in growth and
567 development. *Plant Physiol* **111**, 671-678 (1996).
568 13 Li, J. & Chory, J. A putative leucine-rich repeat receptor kinase involved in
569 brassinosteroid signal transduction. *Cell* **90**, 929-938 (1997).
570 14 Wang, Z. Y., Seto, H., Fujioka, S., Yoshida, S. & Chory, J. BRI1 is a critical
571 component of a plasma-membrane receptor for plant steroids. *Nature* **410**, 380-
572 383, doi:10.1038/35066597 (2001).
573 15 Kinoshita, T. *et al.* Binding of brassinosteroids to the extracellular domain of
574 plant receptor kinase BRI1. *Nature* **433**, 167-171, doi:10.1038/nature03227
575 (2005).
576 16 Hothorn, M. *et al.* Structural basis of steroid hormone perception by the receptor
577 kinase BRI1. *Nature* **474**, 467-471, doi:10.1038/nature10153 (2011).
578 17 She, J. *et al.* Structural insight into brassinosteroid perception by BRI1. *Nature*
579 **474**, 472-476, doi:10.1038/nature10178 (2011).

580 18 Karlova, R. *et al.* The Arabidopsis SOMATIC EMBRYOGENESIS
581 RECEPTOR-LIKE KINASE1 protein complex includes BRASSINOSTEROID-
582 INSENSITIVE1. *Plant Cell* **18**, 626-638, doi:10.1105/tpc.105.039412 (2006).
583 19 Li, J. *et al.* BAK1, an Arabidopsis LRR receptor-like protein kinase, interacts
584 with BRI1 and modulates brassinosteroid signaling. *Cell* **110**, 213-222 (2002).
585 20 Nam, K. H. & Li, J. BRI1/BAK1, a receptor kinase pair mediating
586 brassinosteroid signaling. *Cell* **110**, 203-212 (2002).
587 21 Gou, X. *et al.* Genetic evidence for an indispensable role of somatic
588 embryogenesis receptor kinases in brassinosteroid signaling. *PLoS Genet* **8**,
589 e1002452, doi:10.1371/journal.pgen.1002452 (2012).
590 22 Yin, Y. *et al.* BES1 accumulates in the nucleus in response to brassinosteroids to
591 regulate gene expression and promote stem elongation. *Cell* **109**, 181-191
592 (2002).
593 23 Wang, Z. Y. *et al.* Nuclear-localized BZR1 mediates brassinosteroid-induced
594 growth and feedback suppression of brassinosteroid biosynthesis. *Dev Cell* **2**,
595 505-513 (2002).
596 24 He, J. X., Gendron, J. M., Yang, Y., Li, J. & Wang, Z. Y. The GSK3-like kinase
597 BIN2 phosphorylates and destabilizes BZR1, a positive regulator of the
598 brassinosteroid signaling pathway in Arabidopsis. *Proc Natl Acad Sci U S A* **99**,
599 10185-10190, doi:10.1073/pnas.152342599 (2002).
600 25 He, J. X. *et al.* BZR1 is a transcriptional repressor with dual roles in
601 brassinosteroid homeostasis and growth responses. *Science* **307**, 1634-1638,
602 doi:10.1126/science.1107580 (2005).
603 26 Yin, Y. *et al.* A new class of transcription factors mediates brassinosteroid-
604 regulated gene expression in Arabidopsis. *Cell* **120**, 249-259,
605 doi:10.1016/j.cell.2004.11.044 (2005).
606 27 Kagale, S., Divi, U. K., Krochko, J. E., Keller, W. A. & Krishna, P.
607 Brassinosteroid confers tolerance in Arabidopsis thaliana and Brassica napus to
608 a range of abiotic stresses. *Planta* **225**, 353-364, doi:10.1007/s00425-006-0361-
609 6 (2007).
610 28 Krishna, P. Brassinosteroid-Mediated Stress Responses. *J Plant Growth Regul*
611 **22**, 289-297, doi:10.1007/s00344-003-0058-z (2003).
612 29 Sahni, S. *et al.* Overexpression of the brassinosteroid biosynthetic gene DWF4
613 in Brassica napus simultaneously increases seed yield and stress tolerance. *Sci*
614 *Rep* **6**, 28298, doi:10.1038/srep28298 (2016).
615 30 Feng, Y., Yin, Y. & Fei, S. Down-regulation of BdBRI1, a putative
616 brassinosteroid receptor gene produces a dwarf phenotype with enhanced
617 drought tolerance in Brachypodium distachyon. *Plant Sci* **234**, 163-173,
618 doi:10.1016/j.plantsci.2015.02.015 (2015).
619 31 Ye, H. *et al.* RD26 mediates crosstalk between drought and brassinosteroid
620 signalling pathways. *Nat Commun* **8**, 14573, doi:10.1038/ncomms14573 (2017).
621 32 Zhang, S., Cai, Z. & Wang, X. The primary signaling outputs of brassinosteroids
622 are regulated by abscisic acid signaling. *Proc Natl Acad Sci U S A* **106**, 4543-
623 4548, doi:10.1073/pnas.0900349106 (2009).
624 33 Gui, J. *et al.* OsREM4.1 Interacts with OsSERK1 to Coordinate the Interlinking
625 between Abscisic Acid and Brassinosteroid Signaling in Rice. *Dev Cell* **38**, 201-
626 213, doi:10.1016/j.devcel.2016.06.011 (2016).
627 34 Huang, D., Wu, W., Abrams, S. R. & Cutler, A. J. The relationship of drought-
628 related gene expression in Arabidopsis thaliana to hormonal and environmental
629 factors. *J Exp Bot* **59**, 2991-3007, doi:10.1093/jxb/ern155 (2008).

630 35 Chung, Y., Kwon, S. I. & Choe, S. Antagonistic regulation of Arabidopsis
631 growth by brassinosteroids and abiotic stresses. *Mol Cells* **37**, 795-803,
632 doi:10.14348/molcells.2014.0127 (2014).
633 36 Vilarrasa-Blasi, J. *et al.* Regulation of plant stem cell quiescence by a
634 brassinosteroid signaling module. *Dev Cell* **30**, 36-47,
635 doi:10.1016/j.devcel.2014.05.020 (2014).
636 37 Lozano-Elena, F., Planas-Riverola, A., Vilarrasa-Blasi, J., Schwab, R. & Caño-
637 Delgado, A. I. Paracrine brassinosteroid signaling at the stem cell niche controls
638 cellular regeneration. *Journal of Cell Science* **131**, doi:10.1242/jcs.204065
639 (2018).
640 38 Fàbregas, N. & Caño-Delgado, A. I. Turning on the microscope turret: a new
641 view for the study of brassinosteroid signaling in plant development. *Physiol*
642 *Plant* **151**, 172-183, doi:10.1111/ppl.12130 (2014).
643 39 Friedrichsen, D. M., Joazeiro, C. A., Li, J., Hunter, T. & Chory, J.
644 Brassinosteroid-insensitive-1 is a ubiquitously expressed leucine-rich repeat
645 receptor serine/threonine kinase. *Plant Physiol* **123**, 1247-1256 (2000).
646 40 Caño-Delgado, A. *et al.* BRL1 and BRL3 are novel brassinosteroid receptors
647 that function in vascular differentiation in Arabidopsis. *Development* **131**, 5341-
648 5351, doi:10.1242/dev.01403 (2004).
649 41 Fàbregas, N. *et al.* The brassinosteroid insensitive1-like3 signalosome complex
650 regulates Arabidopsis root development. *Plant Cell* **25**, 3377-3388,
651 doi:10.1105/tpc.113.114462 (2013).
652 42 Belkhadir, Y. & Jaillais, Y. The molecular circuitry of brassinosteroid signaling.
653 *New Phytol* **206**, 522-540, doi:10.1111/nph.13269 (2015).
654 43 Eremina, M. *et al.* Brassinosteroids participate in the control of basal and
655 acquired freezing tolerance of plants. *Proc Natl Acad Sci U S A* **113**, E5982-
656 E5991, doi:10.1073/pnas.1611477113 (2016).
657 44 Nakamura, A. *et al.* The role of OsBRI1 and its homologous genes, OsBRL1
658 and OsBRL3, in rice. *Plant Physiol* **140**, 580-590, doi:10.1104/pp.105.072330
659 (2006).
660 45 Vragovic, K. *et al.* Translatome analyses capture of opposing tissue-specific
661 brassinosteroid signals orchestrating root meristem differentiation. *Proc Natl*
662 *Acad Sci U S A* **112**, 923-928, doi:10.1073/pnas.1417947112 (2015).
663 46 González-García, M. P. *et al.* Brassinosteroids control meristem size by
664 promoting cell cycle progression in Arabidopsis roots. *Development* **138**, 849-
665 859, doi:10.1242/dev.057331 (2011).
666 47 Albrecht, C., Russinova, E., Kemmerling, B., Kwaaitaal, M. & de Vries, S. C.
667 Arabidopsis SOMATIC EMBRYOGENESIS RECEPTOR KINASE proteins
668 serve brassinosteroid-dependent and -independent signaling pathways. *Plant*
669 *Physiol* **148**, 611-619, doi:10.1104/pp.108.123216 (2008).
670 48 Hacham, Y. *et al.* Brassinosteroid perception in the epidermis controls root
671 meristem size. *Development* **138**, 839-848, doi:10.1242/dev.061804 (2011).
672 49 Duan, Y. *et al.* An endoplasmic reticulum response pathway mediates
673 programmed cell death of root tip induced by water stress in Arabidopsis. *New*
674 *Phytol* **186**, 681-695, doi:10.1111/j.1469-8137.2010.03207.x (2010).
675 50 Takahashi, N., Goto, N., Okada, K. & Takahashi, H. Hydrotropism in abscisic
676 acid, wavy, and gravitropic mutants of Arabidopsis thaliana. *Planta* **216**, 203-
677 211, doi:10.1007/s00425-002-0840-3 (2002).

678 51 Galvan-Ampudia, C. S. *et al.* Halotropism is a response of plant roots to avoid a
679 saline environment. *Curr Biol* **23**, 2044-2050, doi:10.1016/j.cub.2013.08.042
680 (2013).
681 52 Nagata, N., Min, Y. K., Nakano, T., Asami, T. & Yoshida, S. Treatment of dark-
682 grown Arabidopsis thaliana with a brassinosteroid-biosynthesis inhibitor,
683 brassinazole, induces some characteristics of light-grown plants. *Planta* **211**,
684 781-790 (2000).
685 53 Singh, T. N., Aspinall, D. & Paleg, L. G. Proline accumulation and varietal
686 adaptability to drought in barley: a potential metabolic measure of drought
687 resistance. *Nat New Biol* **236**, 188-190 (1972).
688 54 Szabados, L. & Savoure, A. Proline: a multifunctional amino acid. *Trends Plant*
689 *Sci* **15**, 89-97, doi:10.1016/j.tplants.2009.11.009 (2010).
690 55 Krasensky, J. & Jonak, C. Drought, salt, and temperature stress-induced
691 metabolic rearrangements and regulatory networks. *J Exp Bot* **63**, 1593-1608,
692 doi:10.1093/jxb/err460 (2012).
693 56 Urano, K. *et al.* Characterization of the ABA-regulated global responses to
694 dehydration in Arabidopsis by metabolomics. *Plant J* **57**, 1065-1078,
695 doi:10.1111/j.1365-313X.2008.03748.x (2009).
696 57 Durand, M. *et al.* Water Deficit Enhances C Export to the Roots in Arabidopsis
697 thaliana Plants with Contribution of Sucrose Transporters in Both Shoot and
698 Roots. *Plant Physiology* **170**, 1460-1479, doi:10.1104/pp.15.01926 (2016).
699 58 Conrath, U., Pieterse, C. M. & Mauch-Mani, B. Priming in plant-pathogen
700 interactions. *Trends Plant Sci* **7**, 210-216 (2002).
701 59 Ding, Y., Fromm, M. & Avramova, Z. Multiple exposures to drought 'train'
702 transcriptional responses in Arabidopsis. *Nat Commun* **3**, 740,
703 doi:10.1038/ncomms1732 (2012).
704 60 Conesa, A., Nueda, M. J., Ferrer, A. & Talon, M. maSigPro: a method to
705 identify significantly differential expression profiles in time-course microarray
706 experiments. *Bioinformatics* **22**, 1096-1102, doi:10.1093/bioinformatics/btl056
707 (2006).
708 61 Brady, S. M. *et al.* A High-Resolution Root Spatiotemporal Map Reveals
709 Dominant Expression Patterns. *Science* **318**, 801 (2007).
710 62 García-Alcalde, F., García-López, F., Dopazo, J. & Conesa, A. Paintomics: a
711 web based tool for the joint visualization of transcriptomics and metabolomics
712 data. *Bioinformatics* **27**, 137-139, doi:10.1093/bioinformatics/btq594 (2011).
713 63 Shakirova, F. *et al.* Involvement of dehydrins in 24-epibrassinolide-induced
714 protection of wheat plants against drought stress. *Plant Physiology and*
715 *Biochemistry* **108**, 539-548, doi:https://doi.org/10.1016/j.plaphy.2016.07.013
716 (2016).
717 64 Chen, J. *et al.* Arabidopsis WRKY46, WRKY54, and WRKY70 Transcription
718 Factors Are Involved in Brassinosteroid-Regulated Plant Growth and Drought
719 Responses. *The Plant Cell* **29**, 1425 (2017).
720 65 Ge, L.-F. *et al.* Overexpression of the trehalose-6-phosphate phosphatase gene
721 OsTPP1 confers stress tolerance in rice and results in the activation of stress
722 responsive genes. *Planta* **228**, 191-201, doi:10.1007/s00425-008-0729-x (2008).
723 66 Jang, I.-C. *et al.* Expression of a Bifunctional Fusion of the
724 Escherichia coli Genes for Trehalose-6-Phosphate
725 Synthase and Trehalose-6-Phosphate Phosphatase in Transgenic Rice Plants
726 Increases Trehalose Accumulation and Abiotic Stress Tolerance without
727 Stunting Growth. *Plant Physiology* **131**, 516 (2003).

728 67 Nuccio, M. L. *et al.* Expression of trehalose-6-phosphate phosphatase in maize
729 ears improves yield in well-watered and drought conditions. *Nature*
730 *Biotechnology* **33**, 862, doi:10.1038/nbt.3277
731 https://www.nature.com/articles/nbt.3277 - supplementary-information (2015).
732 68 Gu, L. *et al.* ZmGOLS2, a target of transcription factor ZmDREB2A, offers
733 similar protection against abiotic stress as ZmDREB2A. *Plant Molecular*
734 *Biology* **90**, 157-170, doi:10.1007/s11103-015-0403-1 (2016).
735 69 Himuro, Y. *et al.* Arabidopsis galactinol synthase AtGolS2 improves drought
736 tolerance in the monocot model Brachypodium distachyon. *Journal of Plant*
737 *Physiology* **171**, 1127-1131, doi:https://doi.org/10.1016/j.jplph.2014.04.007
738 (2014).
739 70 Selvaraj, M. G. *et al.* Overexpression of an Arabidopsis thaliana galactinol
740 synthase gene improves drought tolerance in transgenic rice and increased grain
741 yield in the field. *Plant Biotechnology Journal* **15**, 1465-1477,
742 doi:10.1111/pbi.12731 (2017).
743 71 Kiyosue, T., Yoshiba, Y., Yamaguchi-Shinozaki, K. & Shinozaki, K. A nuclear
744 gene encoding mitochondrial proline dehydrogenase, an enzyme involved in
745 proline metabolism, is upregulated by proline but downregulated by dehydration
746 in Arabidopsis. *The Plant Cell* **8**, 1323 (1996).
747 72 Nanjo, T. *et al.* Antisense suppression of proline degradation improves tolerance
748 to freezing and salinity in Arabidopsis thaliana. *FEBS Letters* **461**, 205-210,
749 doi:10.1016/S0014-5793(99)01451-9 (1999).
750 73 Wu, C.-y. *et al.* Brassinosteroids Regulate Grain Filling in Rice. *The Plant Cell*
751 **20**, 2130-2145, doi:10.1105/tpc.107.055087 (2008).
752 74 Xu, F., Xi, Z.-m., Zhang, H., Zhang, C.-j. & Zhang, Z.-w. Brassinosteroids are
753 involved in controlling sugar unloading in Vitis vinifera 'Cabernet Sauvignon'
754 berries during véraison. *Plant Physiology and Biochemistry* **94**, 197-208,
755 doi:https://doi.org/10.1016/j.plaphy.2015.06.005 (2015).
756 75 Schroder, F. *et al.* Consequences of induced brassinosteroid deficiency in
757 Arabidopsis leaves. *BMC Plant Biol* **14**, 309, doi:10.1186/s12870-014-0309-0
758 (2014).
759 76 Nishizawa, A., Yabuta, Y. & Shigeoka, S. Galactinol and raffinose constitute a
760 novel function to protect plants from oxidative damage. *Plant Physiol* **147**,
761 1251-1263, doi:10.1104/pp.108.122465 (2008).
762 77 Salazar-Henao, J. E., Lehner, R., Betegon-Putze, I., Vilarrasa-Blasi, J. & Cano-
763 Delgado, A. I. BES1 regulates the localization of the brassinosteroid receptor
764 BRL3 within the provascular tissue of the Arabidopsis primary root. *J Exp Bot*
765 **67**, 4951-4961, doi:10.1093/jxb/erw258 (2016).
766 78 Aljanabi, S. M. & Martinez, I. Universal and rapid salt-extraction of high quality
767 genomic DNA for PCR-based techniques. *Nucleic Acids Res* **25**, 4692-4693
768 (1997).
769 79 Betegón-Putze, I., González, A., Sevillano, X., Blasco-Escámez, D. & Caño-
770 Delgado, A. I. MyROOT: A novel method and software for the semi-automatic
771 measurement of plant root length. *bioRxiv* (2018).
772 80 Asami, T. *et al.* Characterization of brassinazole, a triazole-type brassinosteroid
773 biosynthesis inhibitor. *Plant Physiol* **123**, 93-100 (2000).
774 81 Lisec, J., Schauer, N., Kopka, J., Willmitzer, L. & Fernie, A. R. Gas
775 chromatography mass spectrometry-based metabolite profiling in plants. *Nat*
776 *Protoc* **1**, 387-396, doi:10.1038/nprot.2006.59 (2006).

82 Kopka, J. *et al.* GMD@CSB.DB: the Golm Metabolome Database. *Bioinformatics* **21**, 1635-1638, doi:10.1093/bioinformatics/bti236 (2005).
83 Luedemann, A., Strassburg, K., Erban, A. & Kopka, J. TagFinder for the quantitative analysis of gas chromatography--mass spectrometry (GC-MS)-based metabolite profiling experiments. *Bioinformatics* **24**, 732-737, doi:10.1093/bioinformatics/btn023 (2008).
84 Ritchie, M. E. *et al.* limma powers differential expression analyses for RNA-sequencing and microarray studies. *Nucleic Acids Res* **43**, e47, doi:10.1093/nar/gkv007 (2015).
85 Albacete, A. *et al.* Hormonal changes in relation to biomass partitioning and shoot growth impairment in salinized tomato (Solanum lycopersicum L.) plants. *Journal of Experimental Botany* **59**, 4119-4131, doi:10.1093/jxb/ern251 (2008).
86 Yu, X. *et al.* A brassinosteroid transcriptional network revealed by genome-wide identification of BESI target genes in Arabidopsis thaliana. *Plant J* **65**, 634-646, doi:10.1111/j.1365-313X.2010.04449.x (2011).
87 Sun, Y. *et al.* Integration of brassinosteroid signal transduction with the transcription network for plant growth regulation in Arabidopsis. *Dev Cell* **19**, 765-777, doi:10.1016/j.devcel.2010.10.010 (2010).

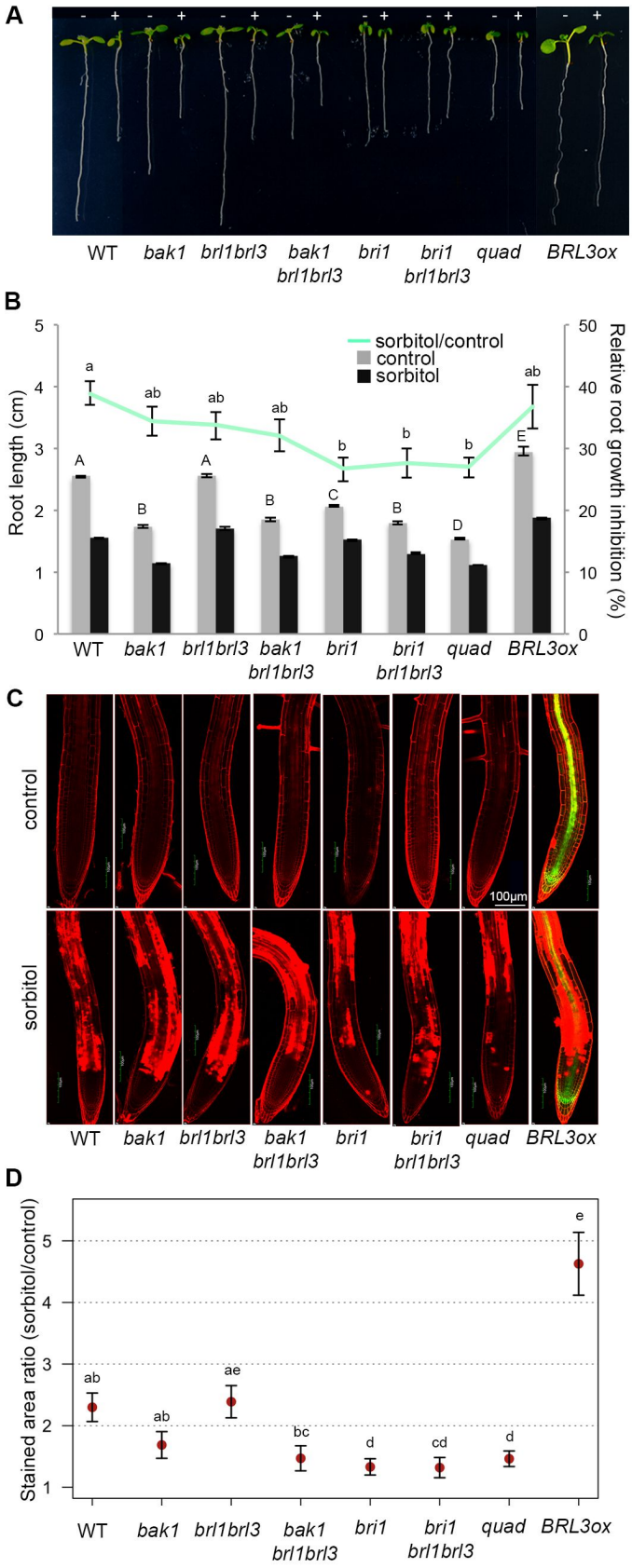

Figure 1. BR perception loss-of-function mutant roots are less sensitive to osmotic stress

Figure 1. BR perception loss-of-function mutant roots are less sensitive to osmotic stress.

(**A**) Seven-day-old roots of WT, BR mutant *bak1*, *brl1brl3, brl1brl3bak1*, *bri1, bri1brl1brl3* and *bri1brl1brl3bak1* (*quad*) and BR overexpressor line *35S:BRL3-GFP (BRL3ox)* grown in control (-) or sorbitol (+) conditions (270mM). (**B**) Seven-day-old root length in control (grey) or sorbitol (black) conditions. Green line depicts relative root growth inhibition upon stress (ratio sorbitol/control root length). Averages of 5 independent biological replicates +/- S.E. (n>150). Different letters mean significant differences in an ANOVA plus Tukey's HSD test. (**C**) Four-day-old roots stained with propidium iodide (PI, red) treated 24h in control (top) or sorbitol (bottom) media. Green channel (GFP) depicts the localization of BRL3 membrane protein receptor under the 35SCaMV constitutive promoter localized in the vascular tissues in primary roots. (**D**) Quantification of cell death in sorbitol-treated root tips. Red dots depict the mean relative PI staining (sorbitol/control) for each genotype. Averages of 5 independent biological replicates +/- S.E. (n>31). Different letters mean significant differences in an ANOVA plus Tukey's HSD test.

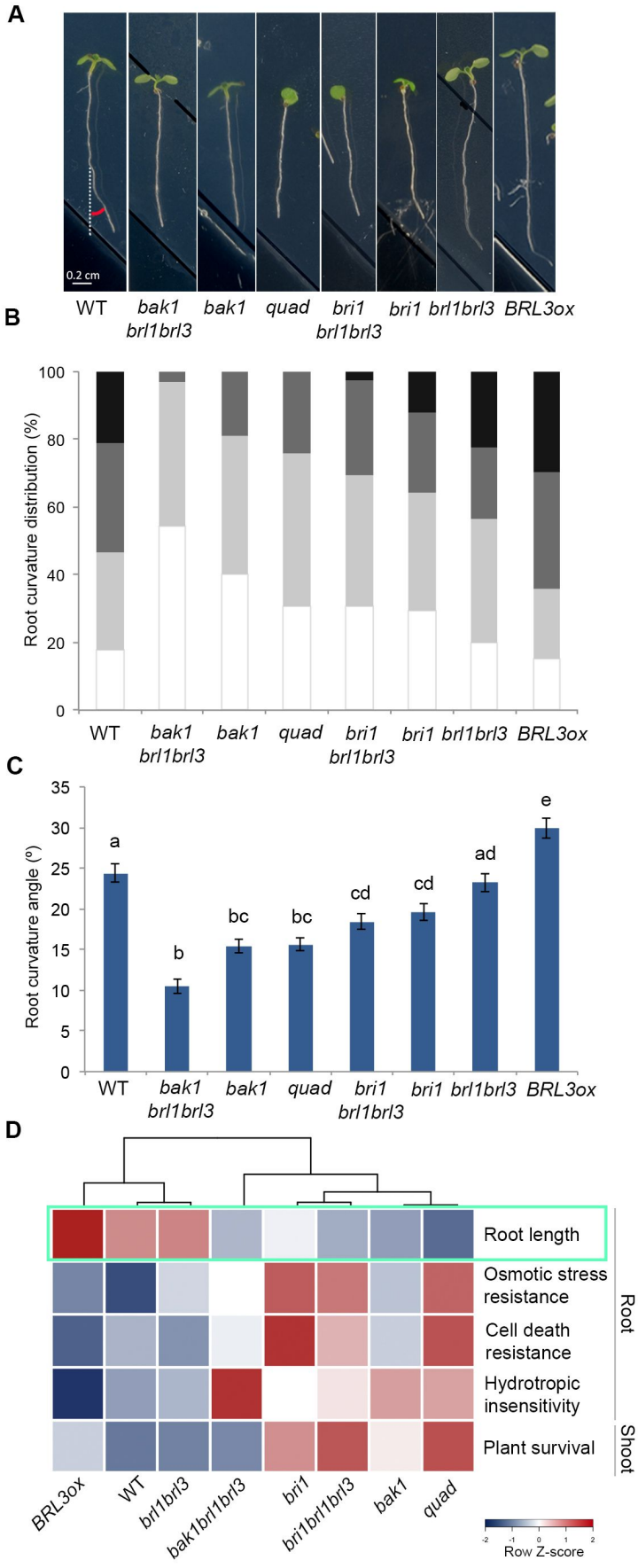

Figure 2. BRL3 receptor signalosome promotes root hydrotropism responses

Figure 2. BRL3 receptor signalosome promotes root hydrotropism responses.

(**A**) Root curvature hydrotropic response in seven-day-old roots after 24h of sorbitol stress induction (270mM). (**B**) Hydrotropic curvature angles distribution. (**C**) Mean values of root curvature angles in WT (24º), *brl1brl3* (23º), *bri1* (20º), *bri1brl1brl3* (18º), *quad* (16º), *bak1* (15º), *br1brl3bak1* (10º) and *BRL3ox* (30º). Averages of 4 independent biological replicates +/- S.E. (n>50). Different letters indicate a significant difference (p-value<0.05) in one-way ANOVA test plus Tukey's HSD test. (**D**) Stress traits matrix for all physiological assays performed on WT, BR loss-of-function mutant and *BRL3ox* roots and shoots. Root growth in control conditions is highlighted in green. Color bar depicts values for scaled data.

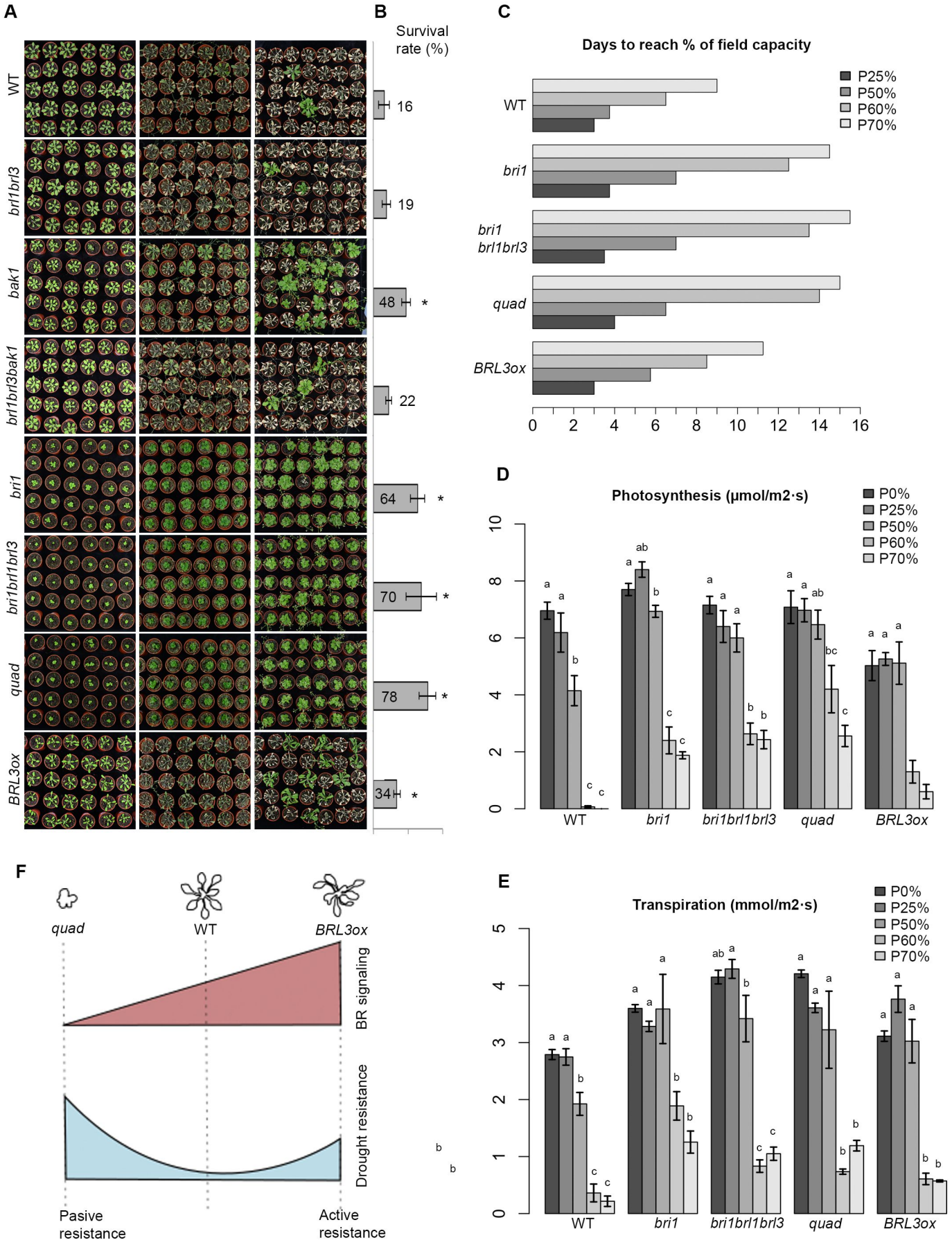

Figure 3. BR perception loss-of-function and overexpression mutants show higher survival rates upon drought stress

Fàbregas et al., MS.

Figure 3. BR perception loss-of-function and overexpression mutants show higher survival rates upon drought stress.

(**A**) From top to bottom, three-week-old plant rosette phenotypes of WT, *brl1brl3, bak1*, *brl1brl3bak1*, *bri1, bri1brl1brl3, quad* and *BRL3ox* grown in well-watered conditions (left column), after 12 days of drought stress (middle column) and plant survival phenotypes after 7 days of re-watering (right column). (**B**) Plant survival rates after 7 days of re-watering. Averages of 5 independent biological replicates +/- S.E. (n>140). Asterisk indicates a significant difference (p-value<0.05) in chi-squared test of mean survival ratios. (**C**) Bar plot shows the days needed to reach different percentages of the soil field capacity for each genotype used in the study. **(D)** Photosynthesis efficiency (µmol/m2*s) at different percentages of field capacity. Bars represent means +/- S.E (n=6). Different letters depict significant differences within each genotype in a one-way ANOVA plus a Tukey's HSD test. **(E**) Transpiration rates (mmol/m2*s) at different percentages of field capacity. Bars represent means +/- S.E (n=6). Different letters depict significant differences within each genotype in a one-way ANOVA plus a Tukey's HSD test. (**F**) Schematic representation on BR signaling level and adult plant size and drought resistance. Loss-of-function mutants avoid the stress passively; whereas plants with increased BRL3 receptors act actively deploying drought stress.

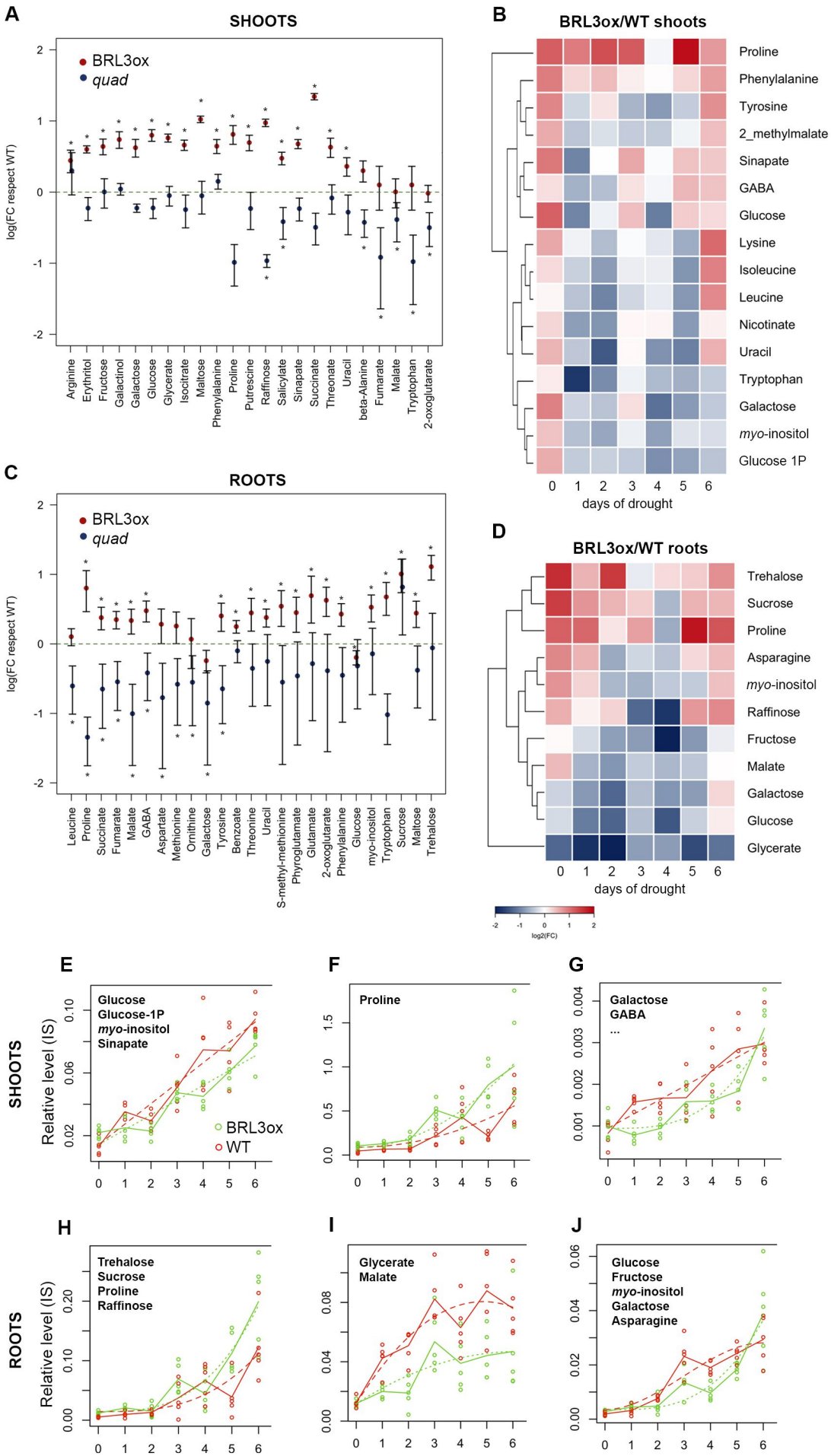

Figure 4. BRL3 overexpression plants show a primed metabolic signature

Fàbregas et al., MS.

Figure 4. BRL3 overexpression plants show a primed metabolic signature.

(**A**) Metabolite profiling of *BRL3ox* shoots in control conditions unveil a significant accumulation of 18 metabolites compared to WT. Metabolite profiling of *quad* shoots in control conditions show significant decreased levels of 7 metabolites compared to WT roots. (**B**) Metabolites following differential dynamics between *BRL3ox* and WT shoots along drought time course. Heatmap represent the log2 ratio of *BRL3ox*/WT. (**C**) Metabolite profiling of *BRL3ox* roots in control conditions unveil a significant accumulation of 20 metabolites compared to WT. Metabolite profiling of *quad* shoots in control conditions show significant decreased levels of 11 metabolites compared to WT roots. (**A-C**) Dotplots represent the means of each metabolite level (in *BRL3ox* and quad) relativized with the median of WT levels +/- S.D. (n=5). Asterisks denote statistical differences in a two-tailed t-test (p-value < 0.05) of the raw data (upper part comparison *BRL3ox* vs. WT, lower part comparison *quad* vs. WT). (**D**) Metabolites following differential dynamics between *BRL3ox* and WT roots along drought time course. Heatmap represent the log2 ratio of *BRL3ox*/WT. (**E-J**) Clustering of the dynamics of metabolite relative levels along drought time course in shoots and roots. Solid lines represent the median profile in the cluster while dashed lines represent the best polynomial curve that fits the data points in the cluster. Statistical significance was evaluated with maSigPro package[92]. (**E**) Metabolites following linear increase in drought in shoots include Glucose, Glucose-1P, myo-inositol and Sinapate. (**F**) Proline follows a stepper exponential increase in *BRL3ox* shoots. (**G**) Metabolites following exponential increase in BRL3ox shoots but linear in WT includes Galactose, GABA, Phenylalanine, Tyrosine, 2-methylmalate, Lysine, Isoleucine, Leucine, Nicotinate, Uracil and Tryptophan. (**H**) Metabolites following steeper exponential increase in *BRL3ox* roots include Trehalose, Sucrose, Proline and Raffinose. (**I**) Metabolites following a reduced linear increase until a maximum in *BRL3ox* roots include Glycerate and Malate. (**J**) Metabolites following exponential increase in *BRL3ox* roots but linear in WT include Glucose, Fructose, *myo*-inositol, Galactose and Asparagine.

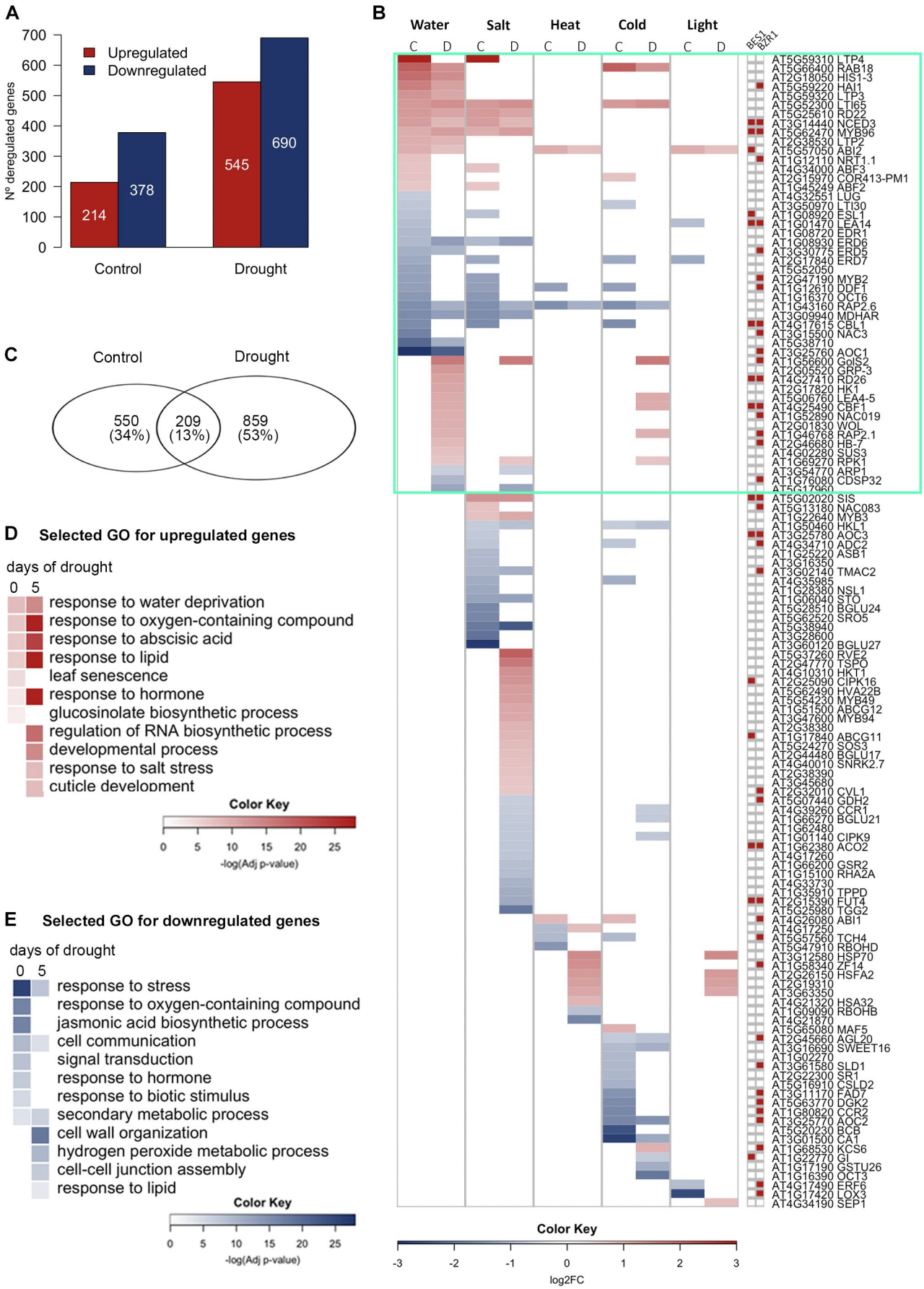

Figure 5. Transcriptomics analysis of BRL3ox roots reveals activated drought stress responses already at basal conditions

Figure 5. Transcriptomics analysis of *BRL3ox* roots reveals activated drought stress responses already at basal conditions

(**A**) Number of genes upregulated or downregulated in control and after five days of water holding. Comparison of *BRL3ox* vs. WT roots. (**B**) Deployment of genes within "Response to stress" (GO:0006950) term that are also annotated as responsive to water, salt, heat, cold and light stress. Colors in the heatmap represent the log2 fold change of BRL3ox roots vs. WT in control (C) or drought (D) conditions. Red color in the squared right-sided heatmaps means that the gene has been previously identified as direct target of BES1 [82],BZR1 [83] transcription factors. (**C**) Overlap between deregulated genes in the control dataset and the drought data set. In both set only overlap a 13% of the total number of deregulated genes. (**D**) Most representative GO categories enriched in *BRL3ox* roots up-regulated genes at time 0 and after 5 days of drought. (**E**) Most representative GO categories enriched in *BRL3ox* roots down-regulated genes at time 0 and after 5 days of drought. Color bars: –log of adjusted p-value (Benjamini-Hochberg).

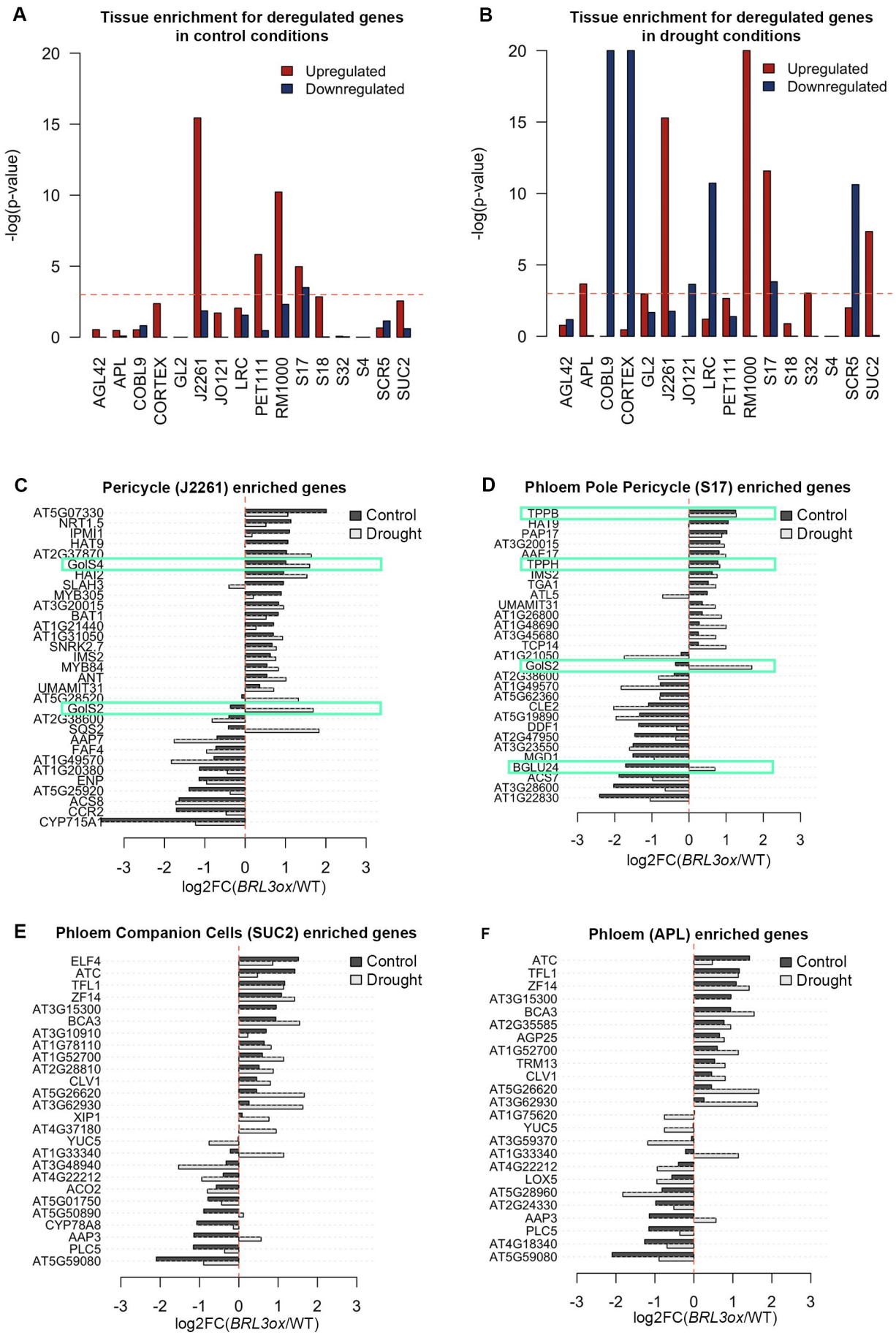

Figure 6. Enrichment of deregulated genes in BRL3ox in the root vasculature

Figure 6. Enrichment of deregulated genes in *BRL3ox* in the root vasculature.

(**A**) Tissue enrichment for upregulated (red) or downregulated (blue) genes in control conditions. Bars trespassing the p-value tresholed (0.05) were considered enriched in the data set. (**B**) Tissue enrichment for upregulated (red) or downregulated (blue) genes after five days of drought. Bars trespassing the p-value tresholed (0.05) were considered enriched in the data set. (**A-B**) Deregulated genes tissue enrichment [59]. AGL42: Quiescent center, APL: Phloem + Companion cells, COBL9: Root hair cells, CORTEX: Cortex, GL2: Non-hair cells, J2661: Pericycle, JO121: Xylem pole pericycle, LRC: Lateral root cap, PET111: Columella, RM1000: Lateral root, S17: Phloem pole pericycle, S18: Maturing Xylem, S32: Protophloem, S4: Developing xylem, SCR5: Endodermis, SUC2: Ploem companion cells. y-axis represent the negative logarithm of one-tailed Fisher's test. (**C**) Genes deregulated enriched in Pericycle (J2261 marker). Blue boxes highlight enzymes involved in the metabolism of deregulated metabolites. (**D**) Genes deregulated enriched in the Phloem Pole Pericycle (S17 marker). Blue boxes highlight enzymes involved in the metabolism of deregulated metabolites. (**E**) Genes deregulated enriched in the Phloem Companion Cells (SUC2 marker). (**F**) Genes deregulated enriched in all Phloem (APL marker). (**C-F**) Bars represent the log2 fold-change of *BRL3ox* vs. WT roots in control (black) or drought conditions (gray).

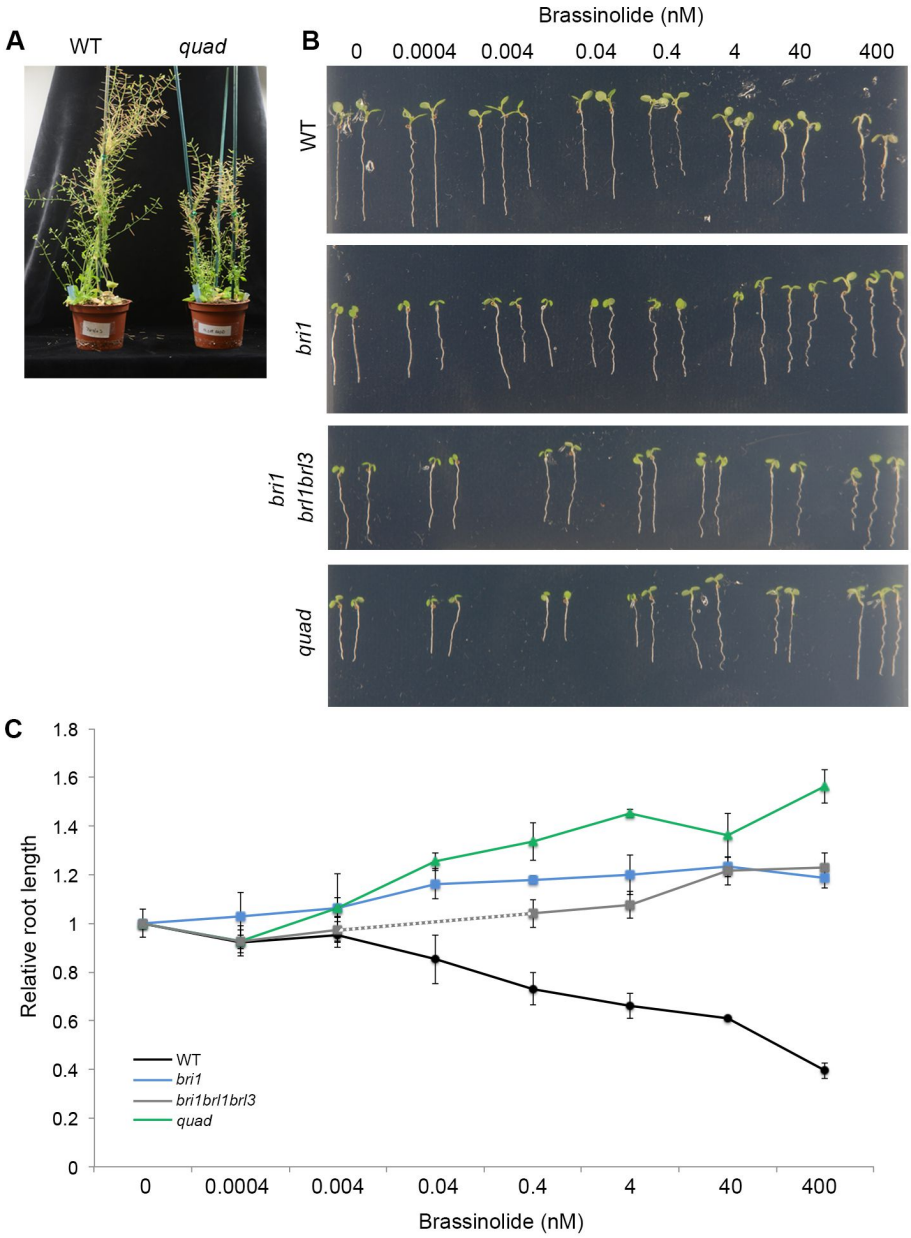

Supplementary Figure 1. BR loss-of-function quad mutant roots are insensitive to BRs

Supplementary Figure 1. BR loss-of-function *quad* mutant roots are insensitive to BRs.

(**A**) Five-week-old *quad* mutants mature plants phenotype. (**B**) Six-day-old roots of WT, *bri1*, *bri1brl1brl3* and *quad* seedlings in a dose-response curve assay at 0.0004, 0.004, 0.04, 0.4, 4, 40 and 400nM of brassinolide (BL) treatment. (**C**) Relative root length of six-day-old WT, *bri1*, *bri1brl1brl3* and *quad* seedlings within BL dose-response curve. Root length in BL was relativized to control root length for each concentration and genotype. BL resistance is observed in *bri1*, *bri1brl1brl3* and *quad* roots. Results are average of three independent biological replicates +/- S.E. (n=100).

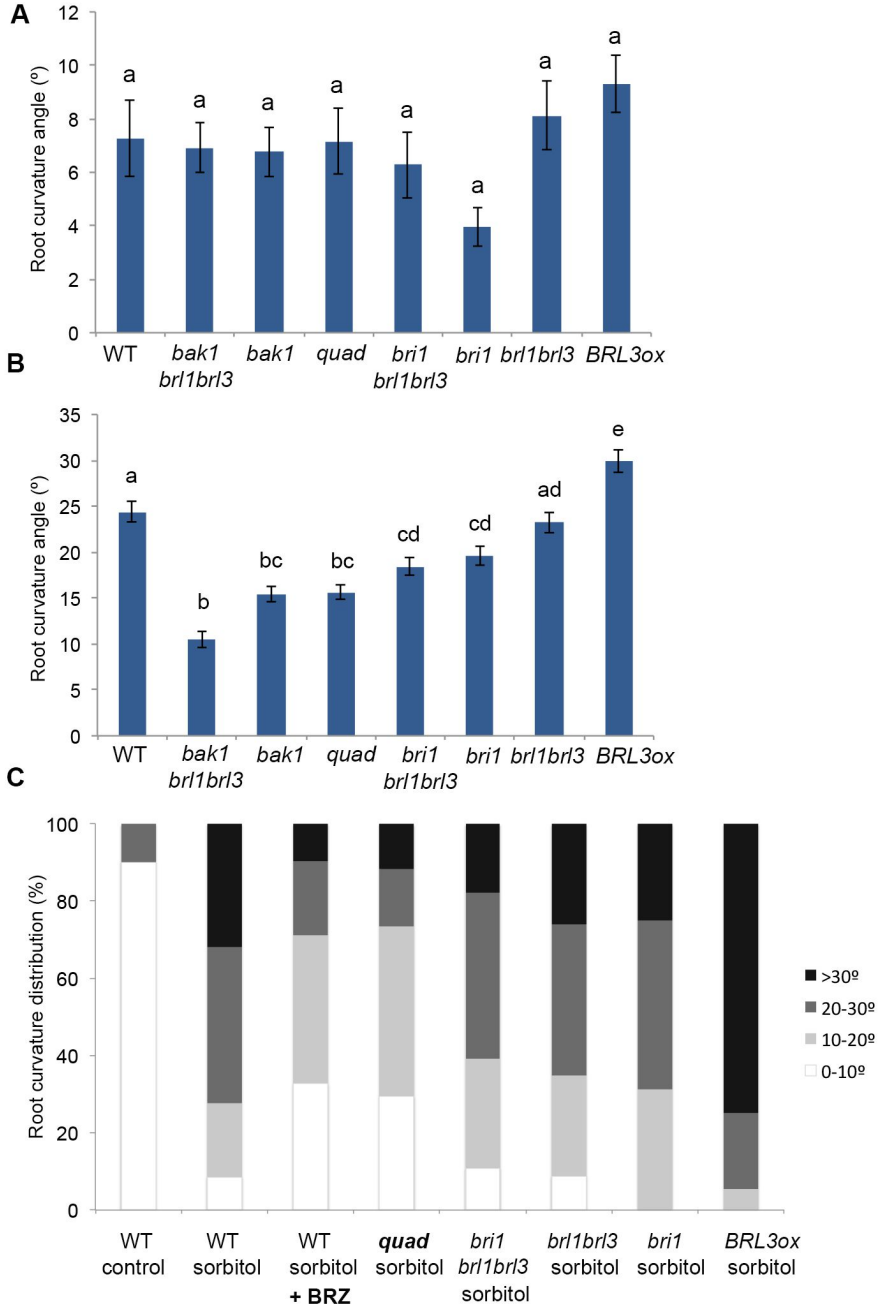

Supplementary Figure 2. BRZ$_{220}$ chemical inhibitor reverts WT root hydrotropic response in sorbitol

Supplementary Figure 2. BRZ_{220} chemical inhibitor reverts WT root hydrotropic response in sorbitol.

(**A**) Curvature angles of roots when the bottom part was replaced with the same media (mock). A small curvature in all genotypes was found (around 7º) but not different from WT. (**B**) Curvature angles of roots when the bottom part was replaced with sorbitol containing media. Note the difference in the scale units with respect A. (**A-B**) Bars represent angle means +/- S.E. (n>50). Different letters mean significant differences in one-way ANOVA plus Tukey's HSD test. (**C**) Distribution graphs of root curvature angles of WT plants in control conditions show 90% of roots curved less than 10º while WT plants treated with 270mM sorbitol show only 8% of roots less than 10º and 68% of roots in between 0 and 30º. Exogenous application of BRZ_{220} reverted the sorbitol-induced response showing 33% of roots curved below 10º and 90% of the roots below 30º, similar to the *quad* mutants insensitive root phenotypes.

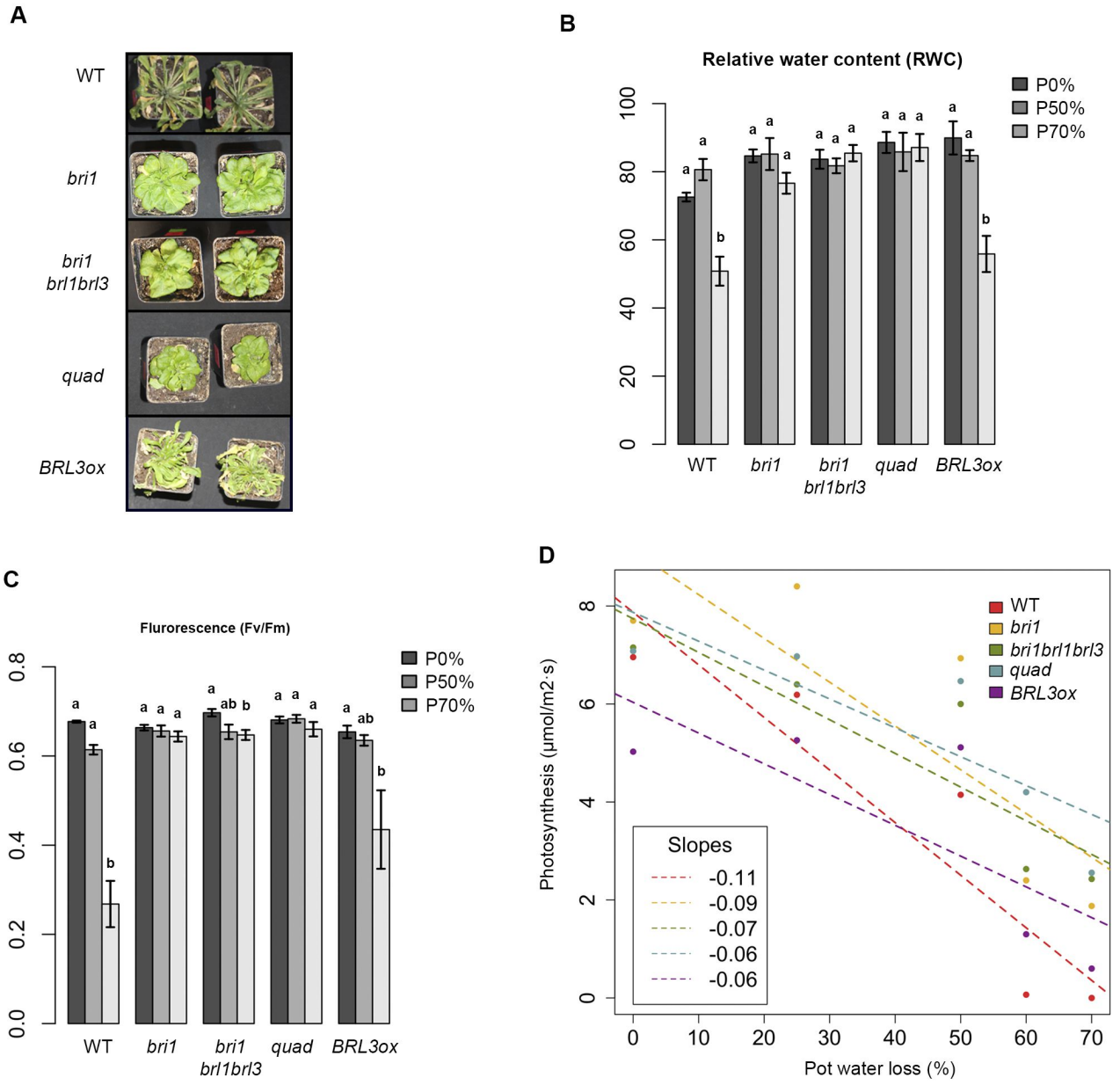

Supplementary Figure 3. Physiological parameters of mature plants under drought stress

Supplementary Figure 3. Physiological parameters of mature plants under drought stress

(**A**) Phenotypes of mature plants after drought. Rosettes were photographed when a 70% of soil water loss was reached (P70%). (**B**) Relative water content (RWC) of mature rosettes at 0% (field capacity), 50% and 70% soil water-loss. (**C**) Photosystem II (PSII) efficiency quantification of mature rosettes at 0% (field capacity), 50% and 70% soil water-loss. (**B-C**) Bars represent means +/- S.E. (n=6). Different letters depict significative differences within each genotype in a one-way ANOVA plus a Tukey's HSD test. (**D**) Plot of photosynthesis efficiency against soil water loss. Data was fitted to lineal model and the slops taken as indicators of drought-induced photosynthesis inhibition. Dots are the means for each genotype and dashed lines the fitted model.

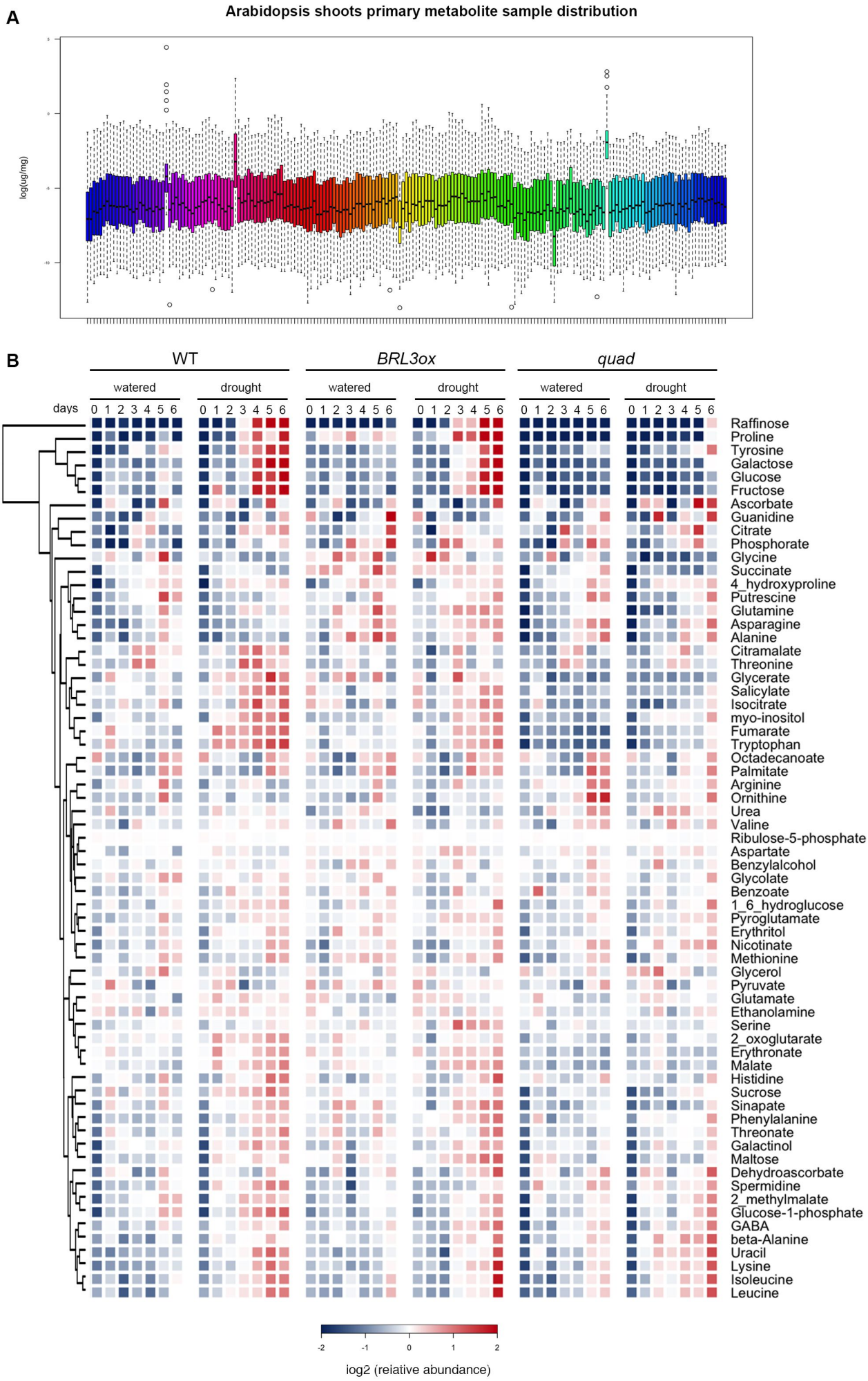

Supplementary Figure 4. WT, BRL3ox and quad mutant metabolite profiling under drought stress in the shoot

Fàbregas et al., MS.

Supplementary Figure 4. WT, *BRL3ox* and *quad* mutant metabolite profiling under drought stress in the shoot

(**A**) Distribution of complete sample set of WT, *BRL3ox* and *quad* shoots within a drought time course. Data show a uniform distribution without normalization. Samples which median was outside the average interquartile range were not considered for further analysis. (**B**) Heat map depicts the metabolic fingerprint of WT, *BRL3ox* and *quad* shoots within time course at control conditions and under drought stress. Homogeneous metabolite relative levels are shown in well-watered conditions, whereas deregulated metabolite patterns appeared upon drought exposure. Color bar depicts row-scaled values for the relative metabolite abundance.

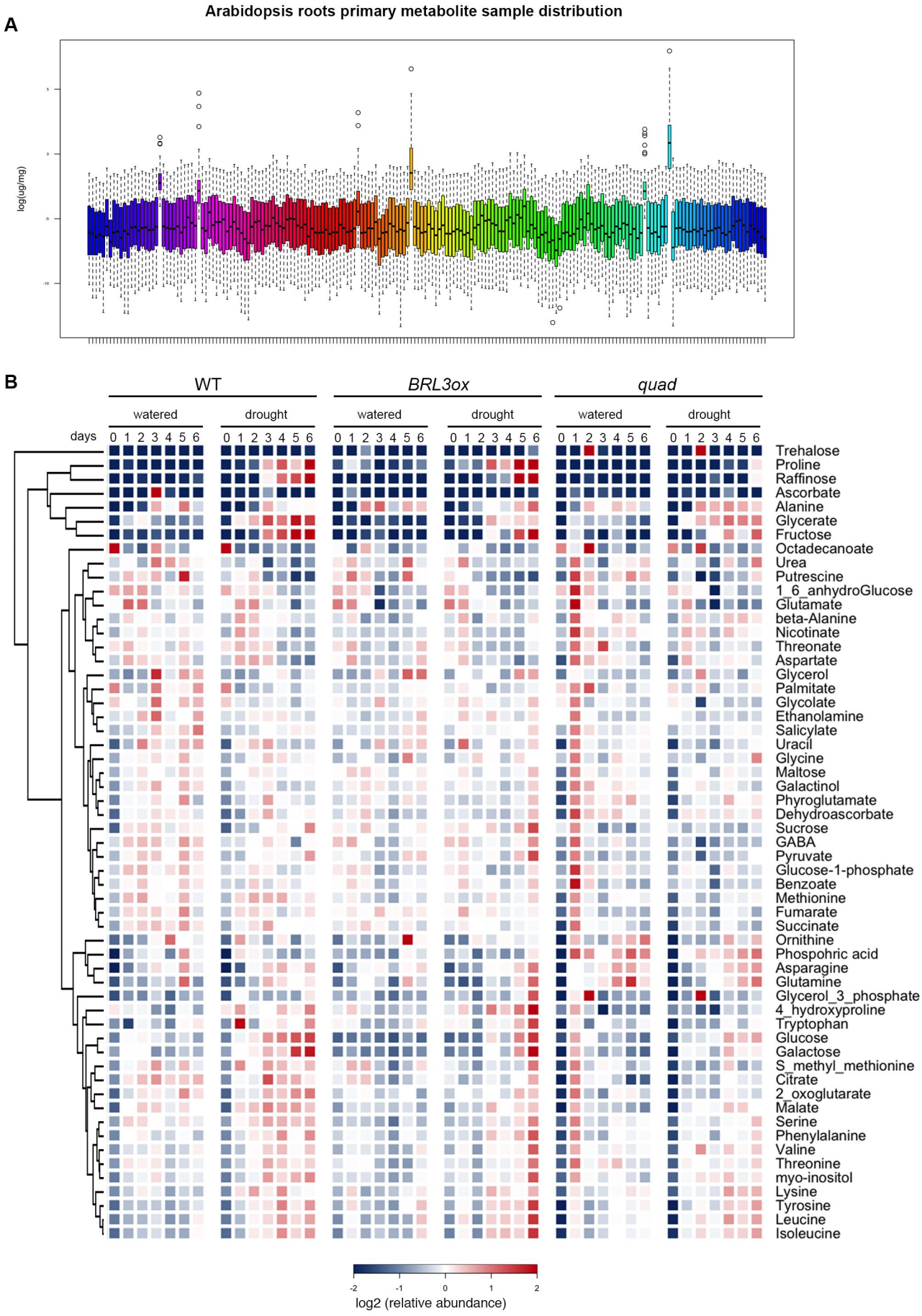

Supplementary Figure 5. WT, BRL3ox and quad mutant metabolite profiling under drought stress in the root

Fàbregas et al., MS.

Supplementary Figure 5. WT, *BRL3ox* and *quad* mutant metabolite profiling under drought stress in the root

(**A**) Distribution of complete sample set of WT, *BRL3ox* and *quad* roots within a drought time course. Data show a uniform distribution without normalization. Samples which median was outside the average interquartile range were not considered for further analysis. (**B**) Heat map depicts the metabolic fingerprint of WT, *BRL3ox* and *quad* roots within time course at control conditions and under drought stress. Homogeneous metabolite relative levels are shown in well-watered conditions, whereas deregulated metabolite patterns appeared upon drought exposure. Color bar depicts row-scaled values for the relative metabolite abundance.

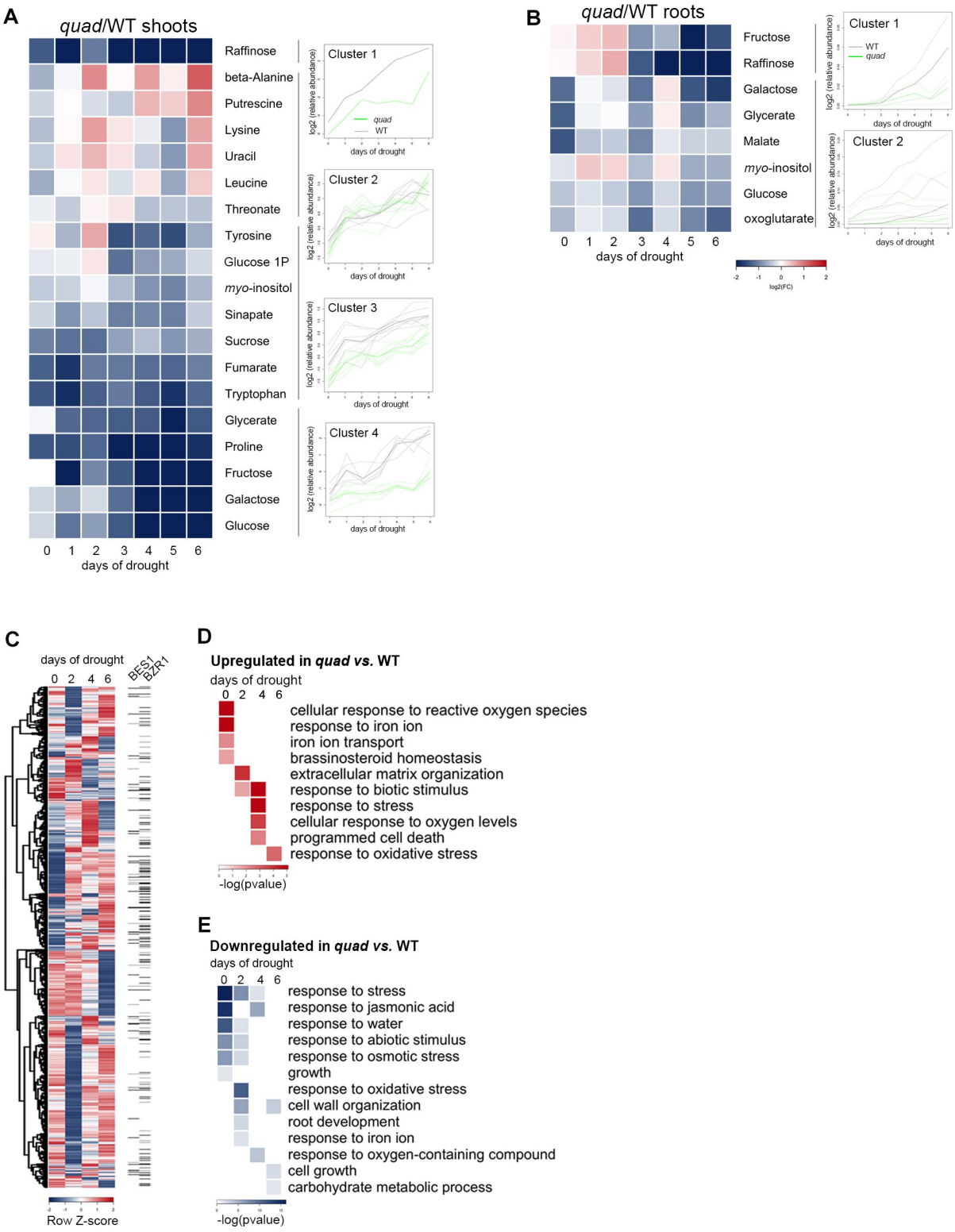

Supplementary Figure 6. Metabolomic and transcriptomics analysis of quad mutants under drought stress

Supplementary Figure 6. Metabolomic and transcriptomics analysis of *quad* mutants under drought stress

(**A**) Metabolites following differential dynamics between *quad* and WT shoots along drought time course. (**B**) Metabolites following differential dynamics between *quad* and WT roots along drought time course. (**A-B**) Clusters summarizing the drought dynamics of a group of metabolites are represented to the right. Heatmap represents the log2 ratio of *quad*/WT. (**C**) Microarray analysis of quad mature rosettes along drought time course. Heatmap represents row-normalized expression values. Black bars columns at the right depict if the gene has been identified as BES1 or BZR1 direct target. (**D**) Representative GO categories enriched among *quad* upregulated genes at 0,2,4 or 6 days of drought. (**E**) Representative GO categories enriched among *quad* upregulated genes at 0,2,4 or 6 days of drought. (**D-E**) Heatmaps represent the –log of corrected p-value for the enrichment (Benjamini-Hochberg).

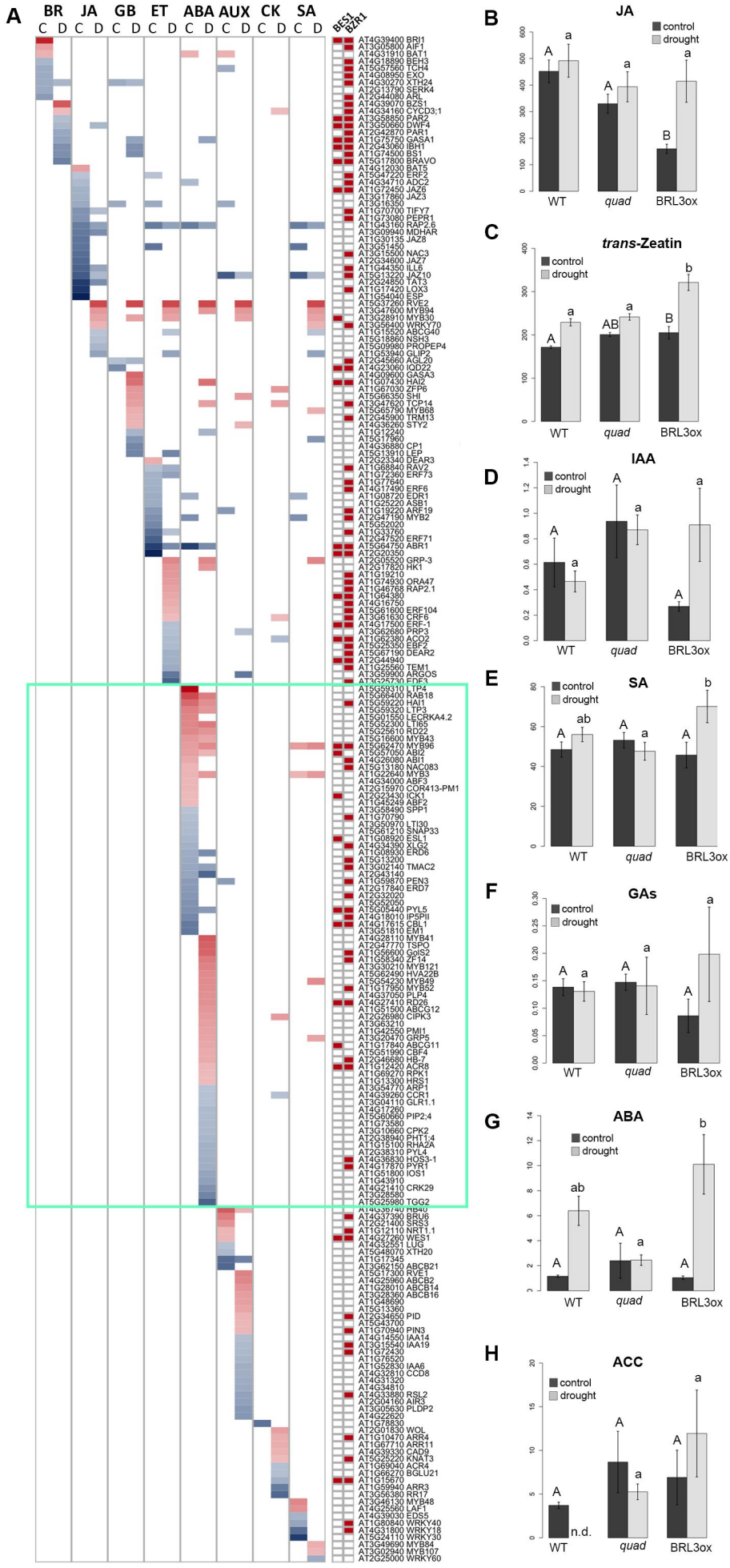

Supplementary Figure 7. Deregulated genes responding to hormones in BRL3ox roots and hormone profiling

Fàbregas et al., MS.

Supplementary Figure 7. Deregulated genes responding to hormones in *BRL3ox* roots and hormone profiling.

(**A**). Deployment of genes within "Response to hormone" (GO:0009725) term that are also annotated as responsive to brassinosteroids (BR), jasmonic acid (JA), gibberelines (GB), ethylene (ET), abscisic acid (ABA), auxin (AUX), citokinin (CK) or salicylic acid (SA). Colors in the heatmap represent the log2 fold change of *BRL3ox* roots vs. WT in control (C) or drought (D) conditions. Red color in the squared right-sided heatmaps means that the gene has been previously identified as direct target of BES1 [82],BZR1 [83] transcription factors. **(B)** Jasmonic acid (JA) levels. **(C)** *trans*-Zeatin levels, a type of cytokinin. (**D**) Indole-3-acetic acid (IAA) levels, the most common auxin. (**E**) Salicylic acid (SA) levels. (**F**) Total gibberellic acid (GAs) levels. (**G**) Abscisic acid (ABA) levels. (**H**) 1-aminocyclopropane-1-carboxylic acid (ACC) levels, a precursor of ethylene biosynthesis. **(B-H)** Data from 5 biological replicates. Error bars denote the average +/- S.E. Different letters indicate a significant difference (p-value<0.05), either in control (capital letters) or drought (lower-case letters) conditions. One-way ANOVA plus Tukey's HSD test.

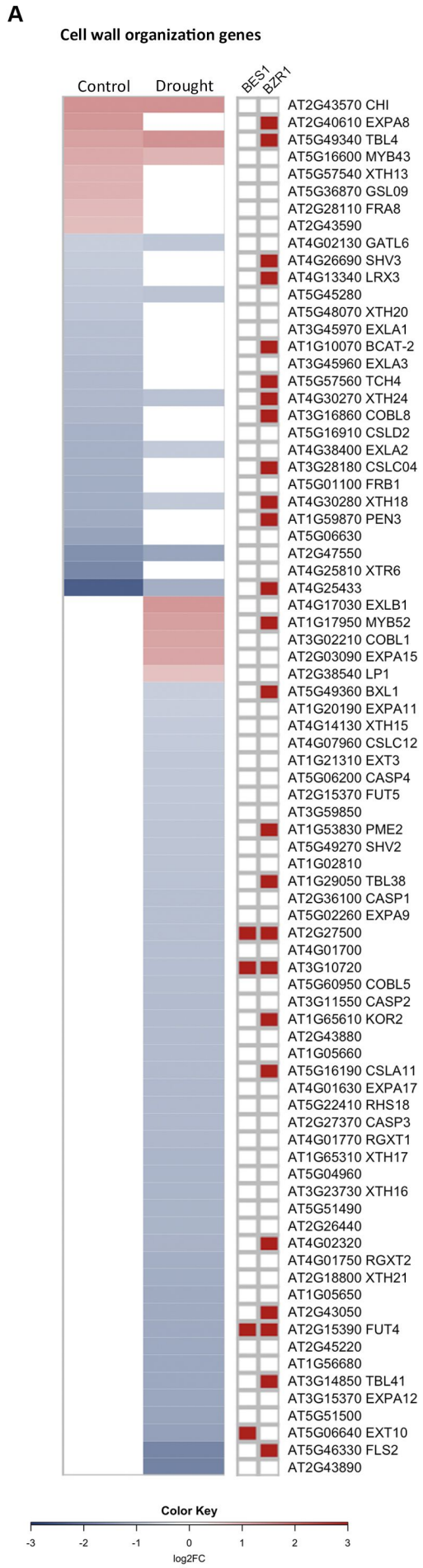

Supplementary Figure 8. Genes of cell wall organization (GO category) deregulated upon drought in BRL3ox roots

Fàbregas et al., MS.

Supplementary Figure 8. Genes of cell wall organization (GO category) deregulated upon drought in *BRL3ox* roots.

(**A**) Deployment of genes within "Cell wall organization" (GO:0071555) term that are deregulated in *BRL3ox* roots in control and drought conditions. Colors in the heatmap represent the log2 fold change of *BRL3ox* roots vs. WT. Red color in the squared right-sided heatmaps means that the gene has been previously identified as direct target of BES1 [82],BZR1 [83] transcription factors

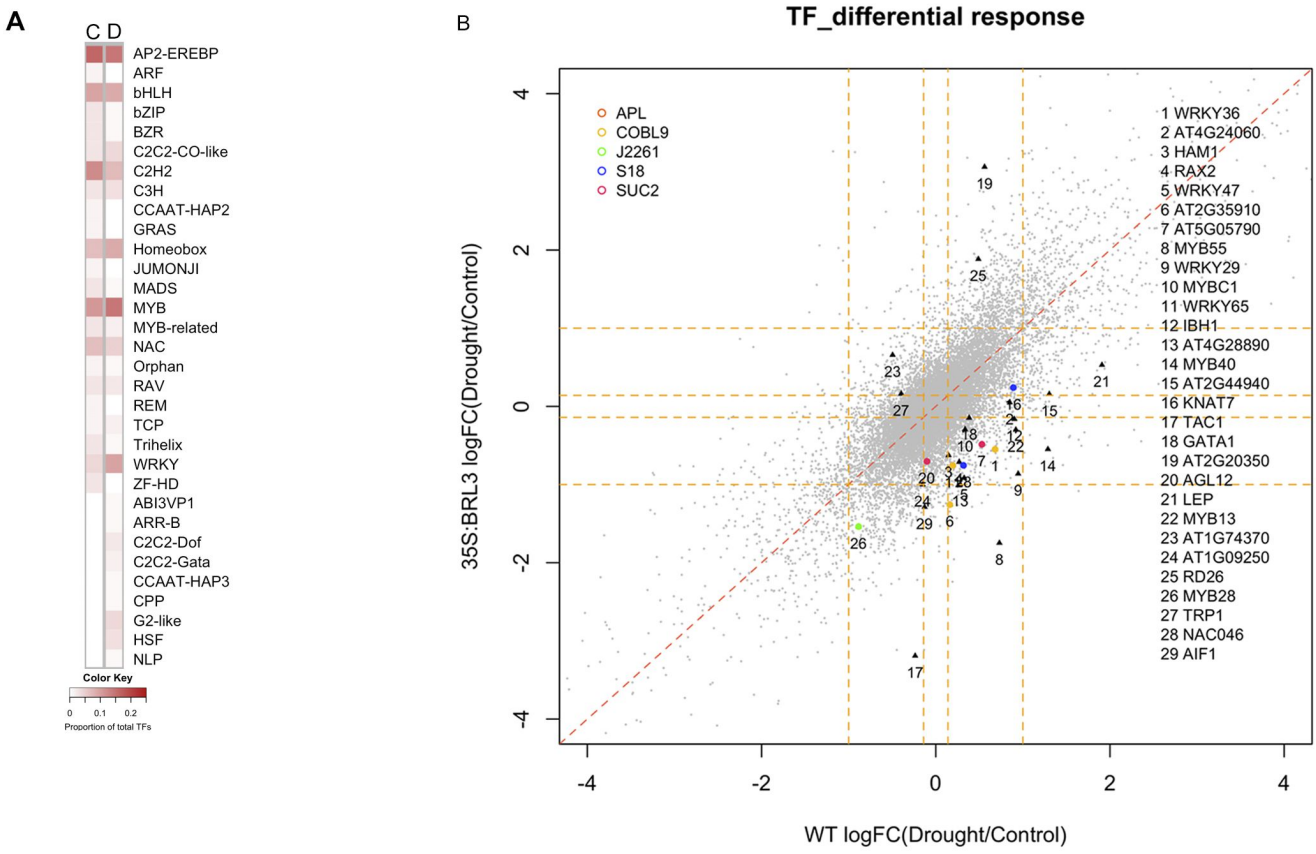

Supplementary Figure 9. Transcription factor analysis of deregulated genes in BRL3ox roots upon drought

Supplementary Figure 9. Transcription factor analysis of deregulated genes in *BRL3ox* roots upon drought.

(**A**) Families of deregulated transcription factors in control (left) and drought (right) conditions. Color key represents the proportion of the family in the total number of deregulated transcription factors. (**B**) Transcription factors with a differential response between *BRL3ox* and WT roots in front of drought (lineal model accounting for interaction). Root tissue-specific [59] transcription factors are denoted in colors; APL: Phloem and phloem companion cells, COBL9: Root hair cells, J2261: Pericycle, S18: Maturing xylem, SUC2: Phloem companions cells.

A

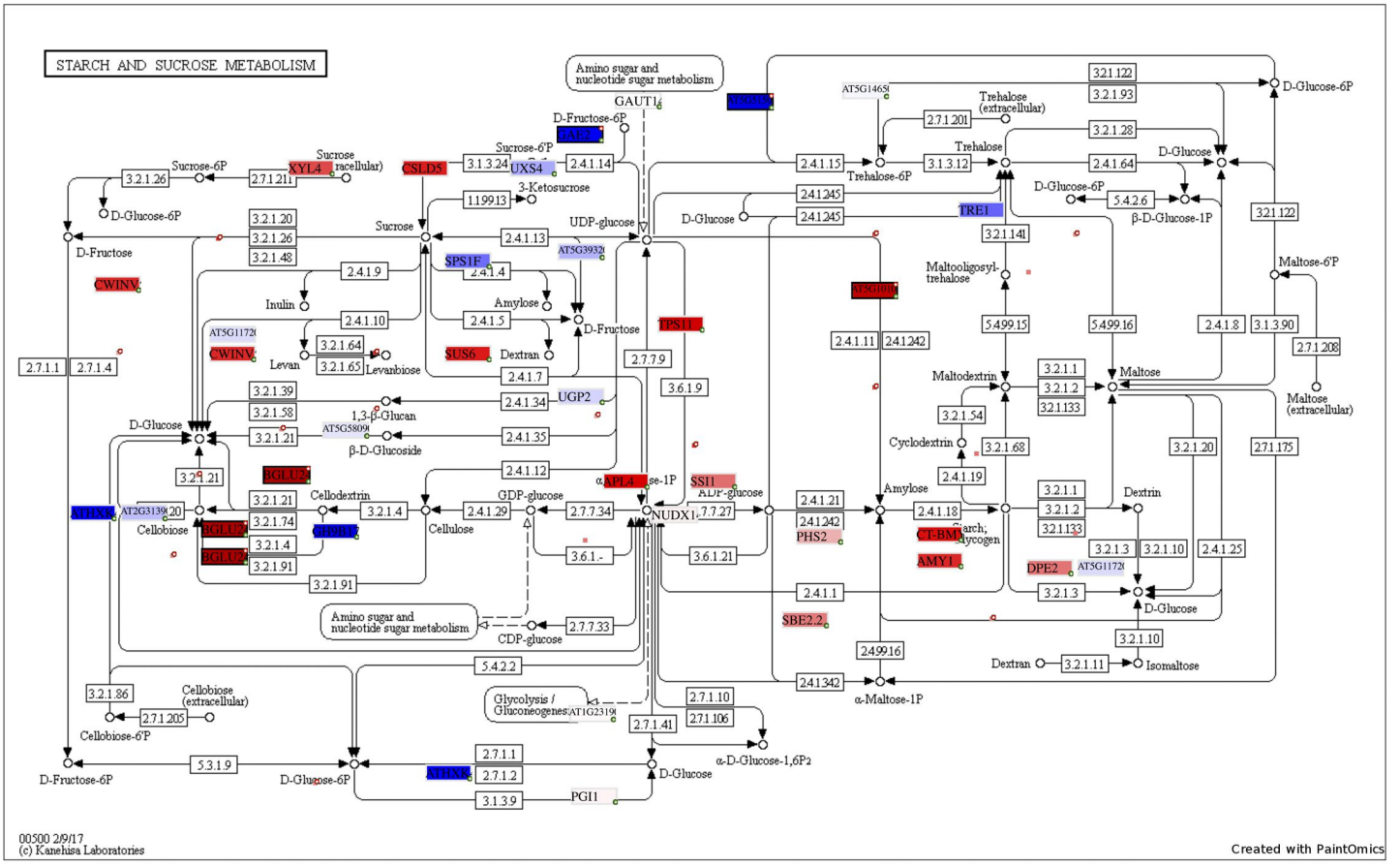

B

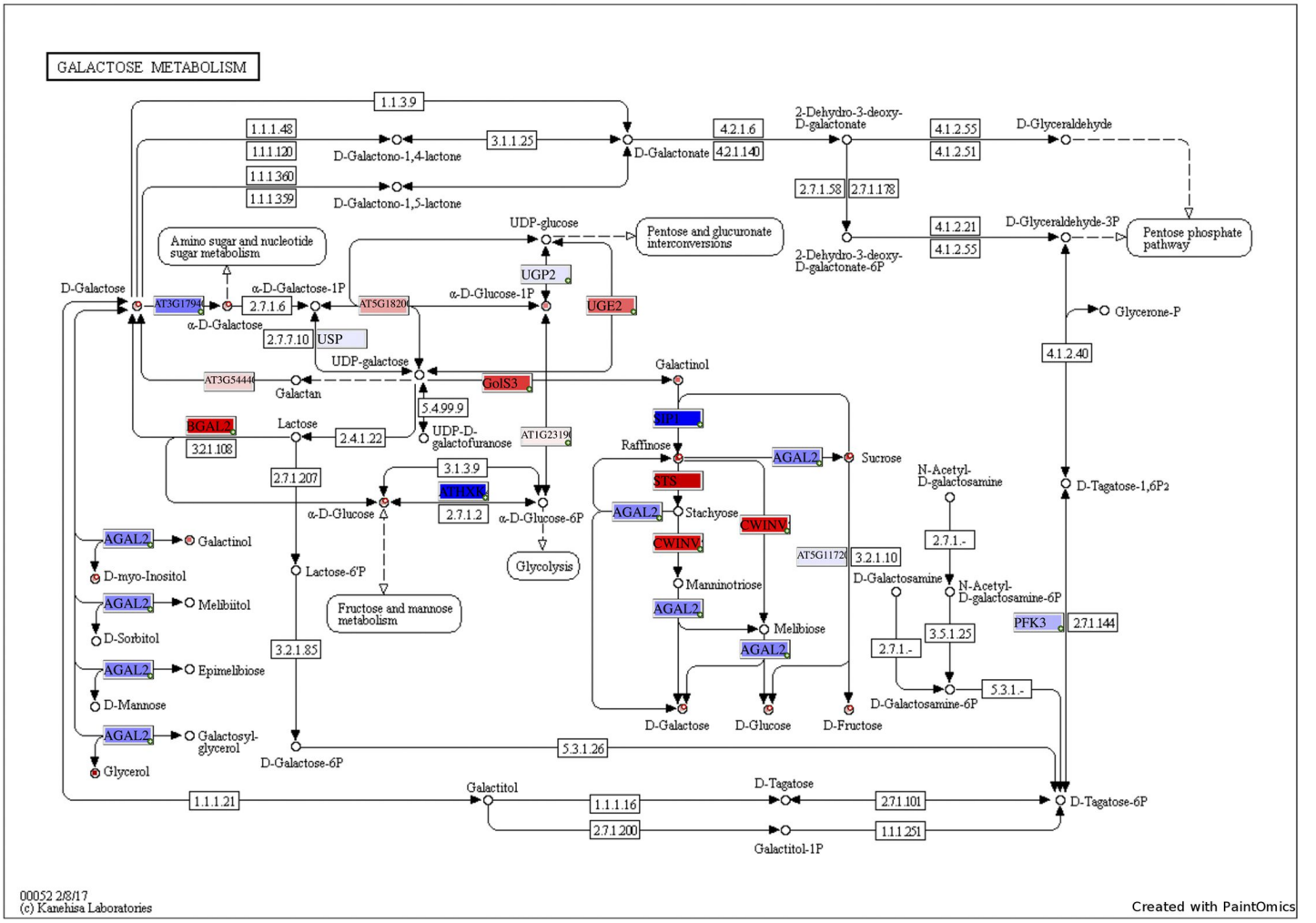

Supplementary Figure 10. Upon drought Sucrose and Galactose metabolic pathways are transcriptionally controlled by BRL3

Fàbregas et al., MS.

Supplementary Figure 10. Upon drought Sucrose and Galactose metabolic pathways are transcriptionally controlled by BRL3.

(**A**) Starch and Sucrose metabolism (KEGG ath00500). Deregulated genes in *BRL3ox* roots are depicted in colored boxes between metabolites. (**B**) Galactose metabolism (KEGG ath00052). Deregulated genes in *BRL3ox* roots are depicted in colored boxes between metabolites. Metabolic pathways with the deregulated enzymes were generated with PaintOmics.

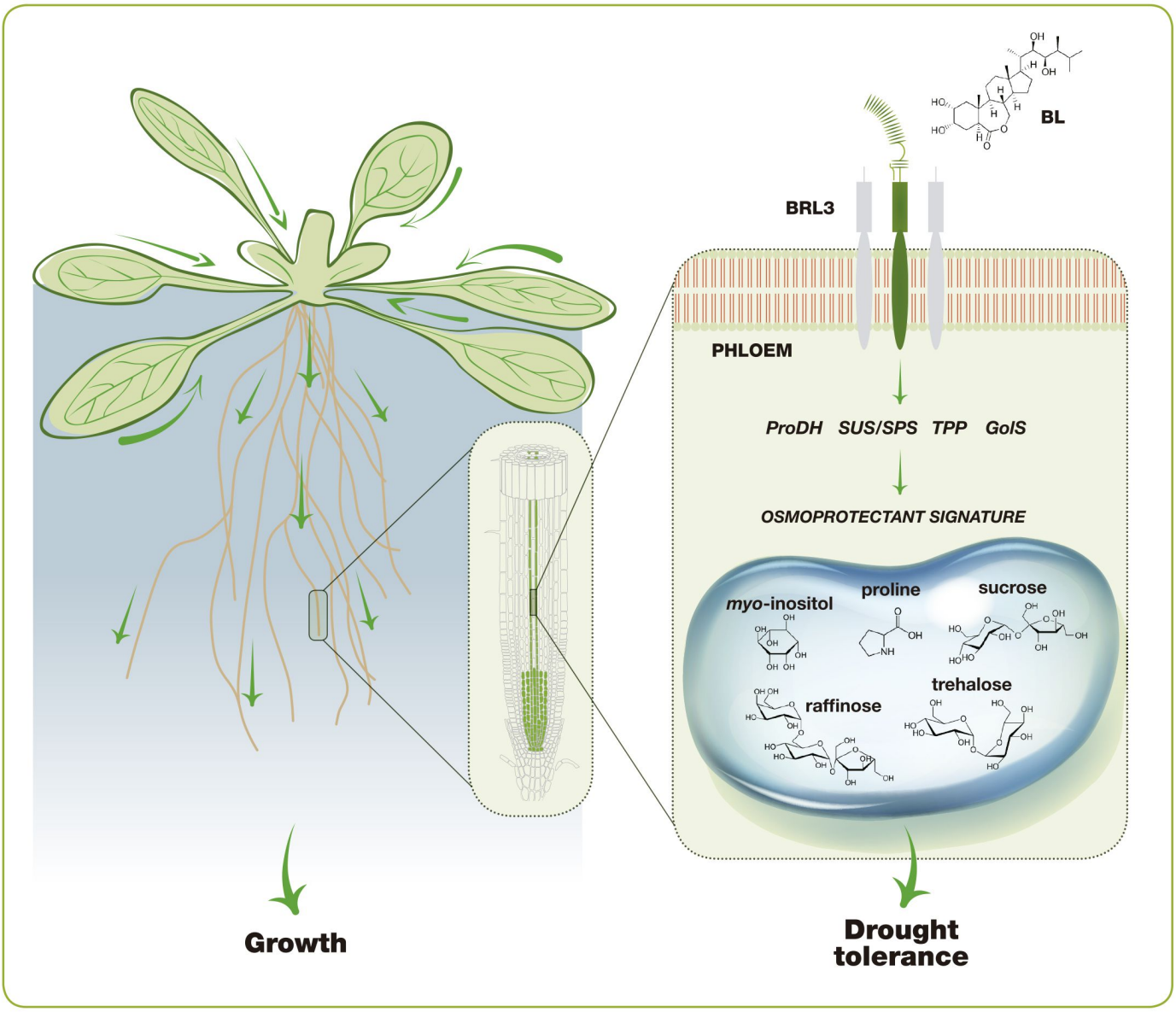

Supplementary Figure 11. Role of vascular BRL3 receptors in drought stress

Supplementary Figure 11. Role of vascular BRL3 receptors in drought stress.

Drought resistance is generally associated to arrested plant growth. Here, we uncover a role for vascular BR receptors in conferring drought tolerance without penalizing overall plant growth. BRL3 receptors are enriched in the vascular (phloem) tissues where they control the division of stem cells. During drought, BRL3 signaling triggers the production of an osmoprotectant metabolic signature that are mobilized to the roots preventing growth arrest during severe drought periods.

A

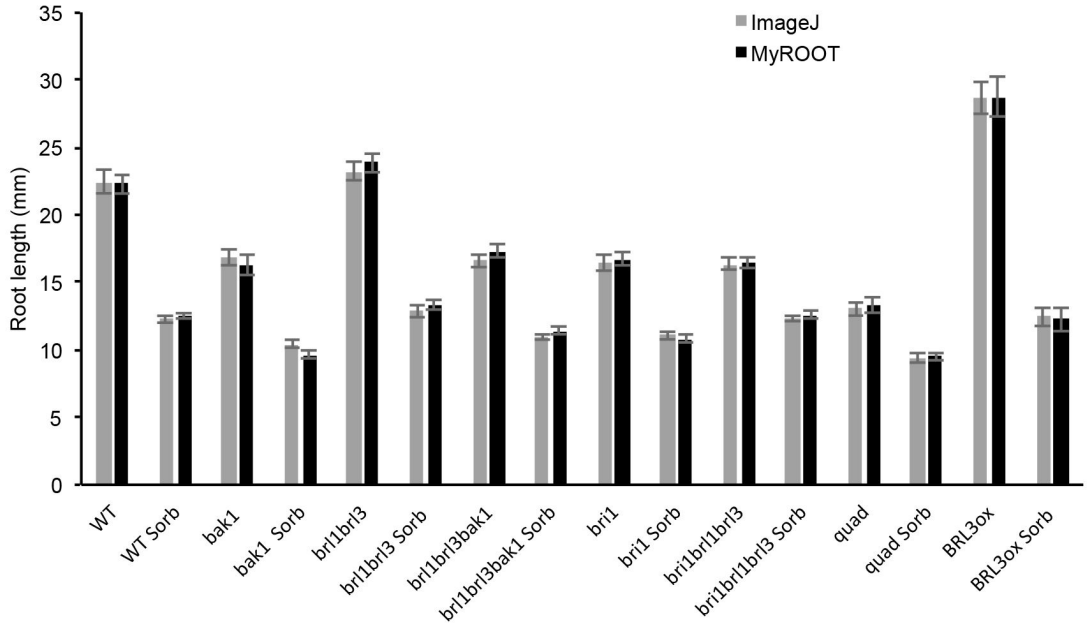

Supplementary Figure 12. Comparison of root length measurements using ImageJ and MyROOT software

Supplementary Figure 12. Comparison of root length measurements using ImageJ and *MyROOT* software.

(**A**) Seven-day-old root length of WT, BR mutants and *BRL3ox* in control and sorbitol (sorb) conditions. Measurements were done manually using ImageJ and compared to data obtained by the semi-automatic software *MyROOT*. No significant differences (t-test, p-value > 0.05) in the mean root lengths were observed between both methods. Bars represent means +/- S.E.